Neurobiology of Disease

Cross-Recognition of a Myelin Peptide by CD8$^+$ T Cells in the CNS Is Not Sufficient to Promote Neuronal Damage

Eva Reuter,[1]* René Gollan,[1]* Nadia Grohmann,[3,4]* Magdalena Paterka,[1,3] Hélène Salmon,[4] Jérôme Birkenstock,[1] Sebastian Richers,[2] Tina Leuenberger,[1,3] Alexander U. Brandt,[3,4] Tanja Kuhlmann,[5] Frauke Zipp,[1,3]† and Volker Siffrin[1,3,4]†

[1]Department of Neurology, Research Center Translational Neurosciences, Rhine Main Neuroscience Network (rmn^2), and [2]Institute of Microanatomy and Neurobiology, University Medical Center of the Johannes Gutenberg University Mainz, 55131 Mainz, Germany, [3]Molecular Neurology Group, Max Delbrueck Center for Molecular Medicine Berlin-Buch, 13125 Berlin, Germany, [4]Charité University Medicine Berlin, ECRC, 13125 Berlin, Germany, and [5]Institute of Neuropathology, University Hospital Münster, 48149 Münster, Germany

Multiple sclerosis (MS) is an inflammatory disease of the CNS thought to be driven by CNS-specific T lymphocytes. Although CD8$^+$ T cells are frequently found in multiple sclerosis lesions, their distinct role remains controversial because direct signs of cytotoxicity have not been confirmed *in vivo*. In the present work, we determined that murine ovalbumin-transgenic (OT-1) CD8$^+$ T cells recognize the myelin peptide myelin oligodendrocyte glycoprotein 40–54 (MOG_{40-54}) both *in vitro* and *in vivo*. The aim of this study was to investigate whether such cross-recognizing CD8$^+$ T cells are capable of inducing CNS damage *in vivo*. Using intravital two-photon microscopy in the mouse model of multiple sclerosis, we detected antigen recognition motility of the OT-1 CD8$^+$ T cells within the CNS leading to a selective enrichment in inflammatory lesions. However, this cross-reactivity of OT-1 CD8$^+$ T cells with MOG peptide in the CNS did not result in clinically or subclinically significant damage, which is different from myelin-specific CD4$^+$ Th17-mediated autoimmune pathology. Therefore, intravital imaging demonstrates that local myelin recognition by autoreactive CD8$^+$ T cells in inflammatory CNS lesions alone is not sufficient to induce disability or increase axonal injury.

Key words: **CD8$^+$ T cells; EAE/MS; intravital microscopy; molecular mimicry**

Introduction

Reports of the presence of CD8$^+$ T cells in multiple sclerosis lesions (Babbe et al., 2000; Siewert et al., 2012) have suggested a crucial role for these cells in the initiation and/or damage processes of the disease (Friese and Fugger, 2009; Huseby et al., 2012). A popular hypothesis for how T cells mediate autoimmunity is molecular mimicry; that is, that infections with certain pathogens drive adaptive immune-cell responses, resulting in cross-recognition of foreign and self-antigens (Benoist and Mathis, 2001). In fact, reports about cross-reactive T cells in multiple sclerosis are frequent, but *in vivo* proof of a causative link to the disease has not yet been found (Cusick et al., 2013).

Specific interaction of CD8$^+$ T cells with target cells requires MHC-I expression, which has long been considered to be absent in the CNS. This paradigm of CNS immune privilege needed correction because MHC-I expression is possible, though tightly regulated in the CNS. Whereas microglia, perivascular macrophages, and endothelial cells constitutively express MHC-I, it is usually below detection limits in astrocytes, oligodendrocytes, and neurons. However, MHC-I has been found to be upregulated in multiple sclerosis lesions on glial cells and neurons in the lesions (Höftberger et al., 2004). For example, strong danger signals under inflammatory conditions, such as the cytokines IFN-γ or TNF-α, also trigger MHC-I expression in neurons (Neumann et al., 1995; Medana et al., 2001). Furthermore, it has been shown that these interactions can have fatal long-term consequences or only transiently affect the neuron (Meuth et al., 2009). Therefore, even though MHC-I expression in CNS tissue is low, specific antigen recognition by CD8$^+$ T cells apparently occurs, although the relevance of this antigen recognition has not yet been clarified. There are also reports of the regulatory roles of CD8$^+$ T cells within the CNS by direct modulation of CD4$^+$ T-cell responses (Jiang et al., 2003; Hu et al., 2004; Zipp and Aktas, 2006).

Recent advances in deep-tissue imaging have made possible the monitoring of immune cells in organotypic environments and the living animal, revealing a direct immune–CNS cell inter-

Received Aug. 6, 2014; revised Jan. 8, 2015; accepted Jan. 15, 2015.

Author contributions: E.R., A.U.B., F.Z., and V.S. designed research; E.R., R.G., N.G., M.P., H.S., J.B., S.R., T.L., T.K., and V.S. performed research; E.R., N.G., A.U.B., and V.S. analyzed data; E.R., F.Z., and V.S. wrote the paper.

This work was supported by the German Research Foundation [DFG; Grant GRK1258 to T.L. and N.G.; Grant SFB-TRR128 to F.Z. (B4), V.S. (B9), and T.K. (Z1); Grant SFB 1080 to FZ (B6)]; the Gemeinnützige Hertie-Stiftung (to V.S.); and the Bundesministerium für Bildung und Forschung (BMBF) (KKNMS; to F.Z.). We thank N. Asselborn, T. Hohnstein, R. Günther, C. Liefländer, and H. Ehrengard for expert technical support and C. Dietz and D. O'Neill for proofreading this manuscript.

The authors declare no competing financial interests.

*E.R., R.G., and N.G. contributed equally to this work.

†F.Z. and V.S. contributed equally to this work.

Correspondence should be addressed to Dr. Volker Siffrin, Klinik und Poliklinik für Neurologie, Universitätsmedizin Mainz, Johannes-Gutenberg, Universität Mainz, Langenbeckstr. 1, 55131 Mainz, Germany. E-mail: siffrinv@gmx.de.

DOI:10.1523/JNEUROSCI.3380-14.2015

 0270-6474/15/354837-14$15.00/0

action (Nitsch et al., 2004; Siffrin et al., 2010). Using two-photon laser scanning microscopy (TPLSM), we have previously shown that activated $CD8^+$ T cells demonstrate characteristic motility changes upon antigen recognition in activated organotypic brain slices, resulting in Ca^{2+} elevation in neurons and neuronal cell death when large amounts of their antigen are applied (Meuth et al., 2009).

In the present study, we identified cross-reactivity of a non-CNS-specific transgenic T-cell receptor (TCR) on $CD8^+$ T cells with a myelin antigen. This cross-reactivity led to characteristic antigen recognition motility of these $CD8^+$ T cell in the CNS both *in vitro* and *in vivo*. Upon transfer of these CNS-cross-reactive $CD8^+$ T cells, we found CNS invasion only in the context of established $CD4^+$ T-cell-initiated experimental autoimmune encephalomyelitis (EAE). However, there was no impact of this cross-recognition on the disease in our *in vivo* animal models of multiple sclerosis, although *in vitro* data clearly proved their cytotoxic potential in the context of the self-antigen.

Materials and Methods

Mice. Ovalbumin-transgenic (OT-1), OT-1xB6.acRFP, OT-1xRag1 $^{-/-}$, *thy1*-EGFPxRag1 $^{-/-}$, 2d2, B6.acRFP, Rag1 $^{-/-}$, *thy1*-TN-XXLxRag1 $^{-/-}$, and C57BL/6J mice were bred under specifically pathogen-free conditions. For adoptive transfer experiments, we used only female animals. For active immunization, equal numbers of male and female animals were used with sex-matched controls. All animal experiments were conducted according to the German Animal Protection Law.

EAE. Mice were immunized subcutaneously with 150 μg of myelin oligodendrocyte glycoprotein 35–55 (MOG_{35-55}; Pepceuticals) emulsified in complete Freund's adjuvant (CFA; BD Difco). Mice received 200 ng of pertussis toxin (List Biological Laboratories) intraperitoneally at the time of immunization and 48 h later.

For adoptive transfer, naive MOG_{35-55} TCR-transgenic 2d2 $CD4^+$ $CD62L^{hi}$ cells were cultured as previously described (Siffrin et al., 2010), and 5×10^6 blasting cells were injected into each Rag1 $^{-/-}$ mouse. Clinical signs of EAE were translated into clinical score as follows: 0, no detectable signs of EAE; 0.5, tail weakness; 1, complete tail paralysis; 2, partial hindlimb paralysis; 2.5, unilateral complete hindlimb paralysis; 3, complete bilateral hindlimb paralysis; 3.5, complete hindlimb paralysis and partial forelimb paralysis; 4, total paralysis of forelimbs and hind limbs (mice with a score >3.5 to be killed); 5, death.

T-cell culture. OT-1, OT-1xRAG1 $^{-/-}$, or OT-1xB6.acRFP mice (6–10 weeks old) were killed and spleen cells were isolated as described previously (Siffrin et al., 2009). Spleen cells were cultured in 3×10^6/ml cell culture medium (RPMI 1640 supplemented with 2 mM L-glutamine, 100 U/ml penicillin, 100 μg/ml streptomycin, and 10% fetal calf serum) and stimulated with the respective peptide [ovalbumin 257–264 ($OVA_{257-264}$) or MOG_{40-54}] in the presence of 10 ng/ml IL-12 and 25 ng/ml IL-18. Cells were kept in cell culture medium supplemented with hrIL-2 (Chiron Therapeutics) for 7 d. Before cells were taken for *in vitro* or *in vivo* experiments, full and comparable activation was ascertained by cytokine production capacity, which was measured on day 7 by FACS after stimulation with anti-CD3/28 antibodies.

Proliferation assay. To measure murine T-cell proliferation, spleen cells from OT-1 mice were isolated and labeled with the fluorescent dye carboxyfluorescein succinimidyl ester (CFSE). T cells were then preincubated for 15–30 min at 37°C in culture medium and subsequently washed twice in prewarmed RPMI + 1% HEPES (RPMI/H). Cells were then resuspended in 10 ml of prewarmed RPMI/H containing 2.5 μM CFSE and incubated for 10 min at 37°C in the dark. The labeled cells were washed twice with cold culture medium, counted, and cultured in 48-well plates for 3 d with different peptides in different concentrations. Cells were harvested, washed with FACS buffer, stained with anti-CD8-APC fluorescent antibody, and measured on a FACSCanto II (BD Germany).

For OT-1xRAG1 $^{-/-}$ T-cell cultures, CFSE-labeled spleen cells of OT-1xRAG1 $^{-/-}$ were mixed in a 1:3 ratio with CD90-depleted irradiated antigen-presenting cells (APCs) from C57BL/6 mouse spleens.

Cytotoxicity assay. The cytotoxicity of OT-1 T cells was assessed as follows: target cells (mouse spleen cells) were labeled with 1 μM CFSE. CFSE labeling was performed as described for proliferation. Target cells were coincubated with OT-1 T cells and antigenic peptides for 20 h. Cells were then harvested and directly transferred to FACS tubes for measurement on the flow cytometer. Immediately before measurement, 1 μl of PI (0.1 μg/μl) was added to each sample to visualize dead and dying cells. Samples were then analyzed on a FACSCanto II and analyzed with the FlowJo software (TreeStar).

Dextramer assay. Antigen specificity was checked by MHC-I/peptide (H-2 Kb/SIINFEKL, H-2 Kb/SIYRYYGL, H-2 Kb/YRSPFSRVVH-LYRNG and H-2 Db/YRSPFSRVVHLYRNG) constructs on a dextrane backbone (produced by Immudex). OT-1 T cells were cultured for 7 d as described above. T cells were harvested, washed with FACS buffer, and stained with a single dextramer. Notably, no peptides were added in this assay. Cells were washed and then stained with anti-CD8 APC. Cells were then analyzed on a FACSCanto II and analyzed with the FlowJo software.

Analysis of steric peptide homology. Structural data for the peptides were obtained from the literature (Clements et al., 2003; Mitaksov et al., 2007). Sequence and structural comparison of the peptides was performed using Universal Protein Resource database/tools (UniProt) and DeepView/Swiss-PdbViewer, Swiss Institute of Bioinformatics, version 4.1.0. Depending on sequence similarities and secondary structure of the peptides, the alignment was reconstructed in 3D. Visualization was optimized subsequently with PyMOL (Incentive Product; DeLano Scientific).

Histology. Mice were killed under deep anesthesia by intracardial perfusion with PBS followed by perfusion with 4% (w/w) paraformaldehyde dissolved in PBS. Spleens, spinal cords, and brains were removed and fixed in 4% paraformaldehyde overnight. Brains were cut at the optic chiasm level and embedded in paraffin together with the spleen and spinal cord. The cervical, thoracic, and higher lumbar spinal cord was cut into 8–11 3-mm-thick transverse segments before embedding. Four-micrometer-thick sections were stained for hematoxylin and eosin, Luxol-fast blue, and periodic acid-Schiff. Immunohistochemistry was performed using an automated immunostainer (Link48; Dako) and an avidin-biotin technique. After deparaffinization, intrinsic peroxidase was blocked by incubation with 3% (v/v) hydrogen peroxide in PBS at 4°C for 20 min. Sections were pretreated for easier antigen retrieval by microwave. The primary antibodies were rat anti-Mac3 (1:200; BD PharMingen) or rat anti-CD3 (1:100; Serotec), rabbit anti-MBP (1:1000; Dako), and neurofilament (1:3000; Abcam). Sections were incubated with secondary biotinylated anti-mouse (ready to use-solution; Dako), anti-rat (1:400; GE Healthcare), or anti-rabbit (1:400; Vector Laboratories) antibodies and avidin-peroxidase (ready to use solution; Dako) for 1 h at room temperature. 3,4-Diaminobenzidine was used as the color substrate and sections were mounted with Eukitt mounting medium after dehydration. MBP staining was performed for analysis of demyelinated areas and neurofilament staining was performed for identification of neuronal/axonal loss. For analysis of axonal loss in EAE lesions, spinal cord slices were analyzed by bright-field microscopy using an Olympus microscope (BX-51) and photographed with an MBF Bioscience camera controlled via the software Stereo Investigator 9 (MBF Bioscience). Pictures of brain lesions and healthy tissue were taken with a 60× oil-immersion objective [1.35 numerical aperture (NA)] and the total area of neurofilament (NF) staining was measured with MBF ImageJ. NF reduction in lesions was determined relative to unaffected brain tissue.

Brain slice two-photon laser scanning microscopy. Four-hundred-micrometer-thick hippocampal slices from C57BL/6 p10–p12 pups were prepared as described previously (Siffrin et al., 2009) and kept in recirculating, hyperoxygenated, and warmed ACSF. T cells were pipetted upon the slice and allowed to enter the slice for ~30 min before imaging; image acquisition was usually performed for ~5 h per slice.

When indicated, antigen $OVA_{257-264}$, $OVA_{323-339}$, or MOG_{40-54} was added through the perfusion. Cells were visualized in acute hippocampal slice cultures by a two-photon system SP2 (Leica) equipped with an upright microscope fitted with a 20× water-immersion objective (NA 0.5; Leica). Cell recognition, cell tracking, and 3D presentation were performed with Volocity (Improvision). Statistical

analysis and graphical presentation were performed with GraphPad Prism 5 software.

Intravital two-photon laser scanning microscopy. Mice were anesthetized and the brainstem exposed as described previously (Siffrin et al., 2010). During surgery and microscopy, body temperature was maintained at 35–37°C. We used near infrared excitation as described previously (Siffrin et al., 2010). Cell recognition, cell tracking, and 3D presentation were performed with Imaris Software (Bitplane). Stratification of tracks as referring to stopping cells (<3 μm/min), swarming cells (≥3 μm/min <6 μm/min), and nonrestricted cell movement (>6 μm/min) has been described previously (Moreau et al., 2012) and was adapted here because of *x*-/*y*-/*z*-drift. Statistical analysis and graphical presentation were performed with GraphPad Prism 5 software.

Ca^{2+} determination. Briefly, the intracellular Ca^{2+} sensor is based on a FRET pair; that is, cerulean fluorescent protein (CFP derivative) as a donor and citrine [yellow fluorescent protein (YFP) derivative] as an acceptor, bound to troponin C in such a way that Ca^{2+}-induced conformation changes of troponin C are directly translated in modifications of the FRET signal; that is, in modifications of the citrine/cerulean ratio. Therefore, relative Ca^{2+} changes can be intravitally visualized in mice, as described previously (Heim et al., 2007; Siffrin et al., 2010), by computing the ratio of citrine emission (535 nm, spectral width 50 nm) and cerulean emission (475 nm, spectral width 40 nm) after excitation at 850 nm. Performing FRET-based calcium titrations, the sensor is very suitable for determining pathological calcium concentrations, although it may not be suitable for resolving very subtle increases in physiological calcium (Mank et al., 2008). The treatment of neuronal tissue with ionomycin leads to the maximal possible saturation (ceiling level) of troponin C with Ca^{2+} in living neurons/axons. Therefore, in all intravital experiments, we related the measured the YFP/CFP ratio to the maximum ratio measured after addition of ionomycin and expressed the relative Ca^{2+} concentration as a percentage of this maximum ratio ($\Delta R/R$ [%]). Thereby, we assumed a linear dependence of the binding affinity of troponin C to Ca^{2+}, as described previously (Heim et al., 2007).

Results

OT-1 T cells can be efficiently activated by MHC-I/$MOG_{40–54}$ because of cross-reactivity of $OVA_{257–264}$ with the myelin peptide $MOG_{40–54}$

OT-1 TCR-transgenic $CD8^+$ T cells recognize an ovalbumin peptide ($OVA_{257–264}$), an antigen that is not expressed in mammalian brains. $MOG_{40–54}$ has been described as a CD8-related self-antigenic epitope of the MOG protein in C57BL/6 mice in the context of EAE and is presented in association with H-2Db (Sun et al., 2003). We found that OT-1 T cells recognized not only their cognate (foreign) antigen $OVA_{257–264}$, but also the myelin peptide $MOG_{40–54}$. We confirmed this cross-recognition or molecular mimicry by three independent read-outs in conventional $CD8^+$ T-cell–peptide–MHC-I recognition assays. First, we checked the proliferative potential of the self- and cross-reactive peptide. OT-1 T cells proliferate vigorously in the presence of the lowest concentrations of $OVA_{257–264}$ (500 pM–50 nM), proving the high avidity of $OVA_{257–264}$/MHC-I/OT-1 TCR complexes. We found that the myelin peptide $MOG_{40–54}$ induced concentration-dependent OT-1 T-cell proliferation (Fig. 1*A*), which showed maximal activation of OT-1 T cells comparable to the cognate $OVA_{257–264}$ at 50 μM $MOG_{40–54}$ (Fig. 1*B*). This antigen concentration is comparable to those known from autoantigens in other contexts (Bettelli et al., 2003; Sun et al., 2003; Perchellet et al., 2004), which have been shown in range of 1–100 μM.

Second, we confirmed the cross-reactivity by proving the cytotoxic potential of $MOG_{40–54}$-activated OT-1 T cells through an APC-based cytotoxicity assay, which showed specific cytotoxicity of OT-1 T cells in the presence of $MOG_{40–54}$ at a dose of 50 μM (Fig. 1*C*), which was the minimal dose needed for maximal proliferation.

Third, we used MHC-I dextramers, fluorescently labeled, ready-to-use MHC-I/peptide multimers that can be used to detect antigen specificity of T cells. We identified specific binding of both $OVA_{257–264}$ and $MOG_{40–54}$ in the context of the MHC-I H-2Kb to OT-1 $CD8^+$ T cells (Fig. 1*D*, top). Control polyclonally activated wild-type $CD8^+$ (pc$CD8^+$) T cells did not show any binding to any of the tested dextramers, which underlines the specificity of OT-1/H-2Kb/$MOG_{40–54}$ binding (Fig. 1*D*, bottom). Steric homology was obvious in the analysis of the TCR binding motif because the secondary structure of the MOG peptide exposed a strongly homologous motif with $OVA_{257–264}$ (Fig. 1*E*). This supports the previously described idea of true molecular mimicry of the TCR binding part of largely nonidentical peptides (Sandalova et al., 2005), in our case $OVA_{257–264}$, which has no strong sequence homology with the MOG peptide. These results prove that cross-recognition of $MOG_{40–54}$ peptide by OT-1 T cells leads to fully activated and functionally similar T cells by both the foreign antigen and the self-antigen, whereas the required doses for the cross-reactive peptide are much higher than for the cognate peptide.

To rule out any artifacts of the peptide synthesis or peptide solving procedures, we investigated several similarly synthesized and dissolved peptides; for example, the control peptide LCMV $gp_{33–40}$ from lymphocytic choriomeningitis virus glycoprotein (cognate peptide of the MHC-I-dependent transgenic TCR P14), which did not induce any proliferation (data not shown). To exclude contamination with nontransgenic TCR chains (recombination with endogenous TCR chains), we performed similar experiments with RAG-$1^{-/-}$ × OT-1 lymphocytes (no endogenous TCR rearrangements), which confirmed correct TCR expression (data not shown).

OT-1 $CD8^+$ T cells, but not OT-2 $CD4^+$ T cells, show antigen recognition motility upon cognate antigen application in organotypic brain slices

To investigate the effects of the cross-recognition of a myelin peptide by OT-1 $CD8^+$ T cells identified *in vitro* within CNS tissue, we used a T-cell/brain slice coculture model (Meuth et al., 2009). We cocultured these organotypic slices with TCR-transgenic $CD8^+$ (OT-1) or $CD4^+$ (OT-2) T cells, which recognize peptides from chicken OVA, a protein that is not expressed in mice. *In vitro*-activated, IFN-γ-producing, and cell tracker (CMTMR)-labeled OT-1 $CD8^+$ T cells (Fig. 2*A*) were transferred onto an acute hippocampal slice, into which they rapidly entered. OT-1 $CD8^+$ T cells (Fig. 2*B*) homogenously exhibited continuous propulsive motility. To identify the effect of antigen presence in the organotypic environment, we added 25 nM $OVA_{257–264}$ peptide (OT-1 cognate antigen) about 60 min after OT-1 $CD8^+$ T cells had entered the slice (Fig. 2*A*, right). Quantitative analysis revealed a strong decrease in instantaneous velocity for OT-1 T cells immediately after antigen application (Fig. 2*C*; for time lapse representation, see also Fig. 2*F*). OT-1 $CD8^+$ T cells showed a highly significant increase in the percentage of cells with stationary motility from 10.3% to 69.4% after OT-1 $OVA_{257–264}$ (CD8-OVA) application (Fig. 2*D*). In contrast, $OVA_{323–339}$ (CD4-OVA) application did not increase the relative number of stationary cells in the OT-2 $CD4^+$ T-cell hippocampal cocultures (Fig. 2*E*). This lack of response of the OT-2 $CD4^+$ T cells is due to the absence of MHC-II molecules in our slices, which in general is necessary for full activation (Neumann et al., 1996; Celli et al., 2007).

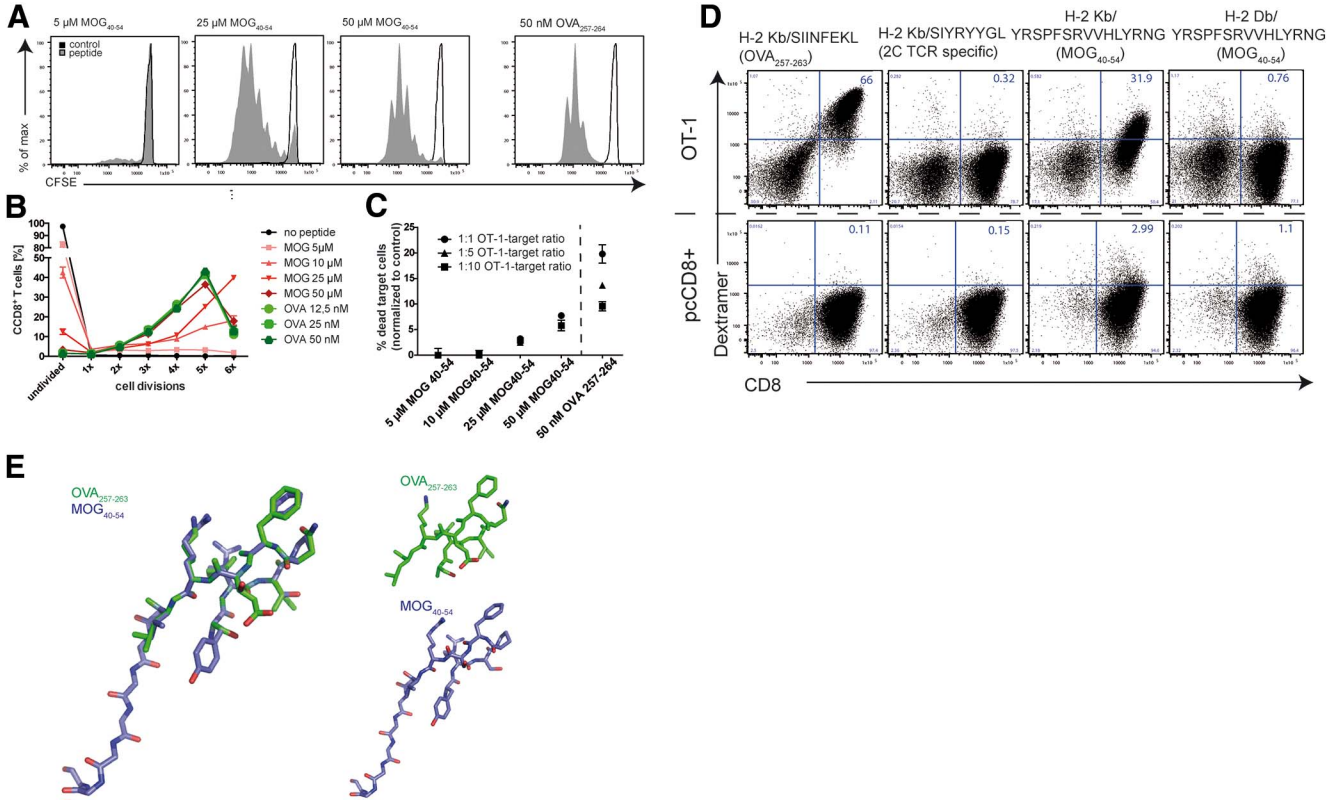

Figure 1. Cross-recognition of the myelin peptide MOG_{40-54} by OT-1 T cells. ***A***, Spleen cells of OT-1 mice were isolated, labeled with CFSE, and then stimulated with different concentrations of antigenic peptides. MOG_{40-54} induced concentration-dependent OT-1 T cell proliferation in this 3D CFSE proliferation assay. The presented data are representative of at least three experiments. ***B***, Quantification of proliferation assays (as shown in ***A***) reveals full activation, that is, comparable activation to stimulation by cognate antigen $OVA_{257-264}$, of OT-1 T cells by a MOG_{40-54} concentration of 50 μM. ***C***, The cytotoxic potential of MOG_{40-54}-activated OT-1 T cells is shown by specific lysis of CFSE-labeled APCs (target cells). PI incorporation in CFSE-positive cells has been analyzed by FACS after 20 h of incubation with preactivated OT-1 T cells and the antigenic peptides; data are representative of at least two independent experiments. ***D***, The specificity of the cross-reactivity of $CD8^+$ OT-1 T cells is confirmed by use of MHC-I-/peptide multimers (dextramers). Specific binding of $OVA_{257-264}$ and MOG_{40-54} is identified in the context of the MHC-I H-2Kb to OT-1 $CD8^+$ T cells. As controls, the 2C TCR-specific dextramer (H-2Kb/SIYRYYGL) and the H-2Db/MOG_{40-54} multimer do not show binding to the OT-1 TCR. Polyclonal $CD8^+$ T cells do not show specific binding of any of the multimers (bottom); data are representative of two independent experiments. ***E***, Structural data of the peptides MOG_{40-54} (purple) and $OVA_{257-264}$ (green) were visualized and compared with DepView/Swiss-PdbViewer (Swiss Institute of Bioinformatics), which showed steric overlap of the central parts of the molecules.

Together, our findings reveal that $CD8^+$ T cells have the potential to recognize their cognate antigen in organotypic CNS tissue and that MHC-I expression in these brain slices is sufficient to induce stopping motility in $CD8^+$ T cells.

OT-1 T cells recognize the myelin peptide MOG_{40-54} in acute hippocampal brain slices

Upon application of $OVA_{257-264}$ or MOG_{40-54} on perfused OT-1 $CD8^+$ T-cell brain slice cocultures, a slowing down to stationary motility was observed under both conditions (Fig. 2*F*). Therefore, we observed cross-recognition of MOG_{40-54} by OT-1 $CD8^+$ T cells, although there was no obvious sequence homology (Fig. 2*G*). The motility changes upon addition of MOG_{40-54} to the OT-1 $CD8^+$ T-cell brain slice cocultures were concentration dependent (Fig. 2*H*,*I*). When MOG_{40-54} was applied at a low concentration of 25 μM (2.5 × cell culture concentration), the mean displacement rate and mean instantaneous velocity showed only a minor reduction, which was in the range of unspecific changes similar to with the control peptide $OVA_{323-339}$ (Fig. 2*H*). In higher dose ranges (200 μM ≈ 20 × cell culture concentration), MOG_{40-54} led to similar changes to the cognate peptide $OVA_{257-264}$ (Fig. 2*C*,*I*). This was in clear contrast to the application of high concentrations of the control peptide (12 μM $OVA_{323-339}$, 20 × cell culture concentration; Fig. 2*H*). For the mean instantaneous velocity, there was a dose-dependent effect of the three tested concentrations (Fig. 2*I*). In this way, we identified a cross-reactivity of the $OVA_{257-264}$-specific OT-1 TCR with MOG_{40-54}.

Transfer of activated OT-1 $CD8^+$ T cells into lymphopenic hosts does not lead to autoimmunity *in vivo*

To investigate the relevance of the observed cross-recognition of a foreign and a self-antigen *in vivo*, we used two separate experimental approaches. In one set of experiments, we injected activated OT-1 T cells (constitutively expressing tdRFP) or, as a control, activated pc$CD8^+$ T cells (constitutively expressing CFP) into naive B6.RAG-$1^{-/-}$ × *thy1*.EGFP mice (lymphopenic mice that express EGFP in axons; Siffrin et al., 2010). The animals were monitored for weight loss for 26 d and clinically evaluated according to EAE function scores. Transfer of activated OT-1 T cells did not lead to any clinical symptoms of disease, not even weight loss, which is the most sensitive sign at the beginning of the disease (Fig. 3*A*). Consistent with this, TPLSM of the brainstem of living, anesthetized mice showed that only a few of the activated OT-1 T cells and control polyclonal (pc) $CD8^+$ T cells were present in the CNS, most likely in the perivascular area (Fig. 3*B*). The transfer of both populations together in one mouse was for reasons of internal control (experimental group: OT-1, control group: wild-type pc$CD8^+$ T cells) in TPLSM. This is neces-

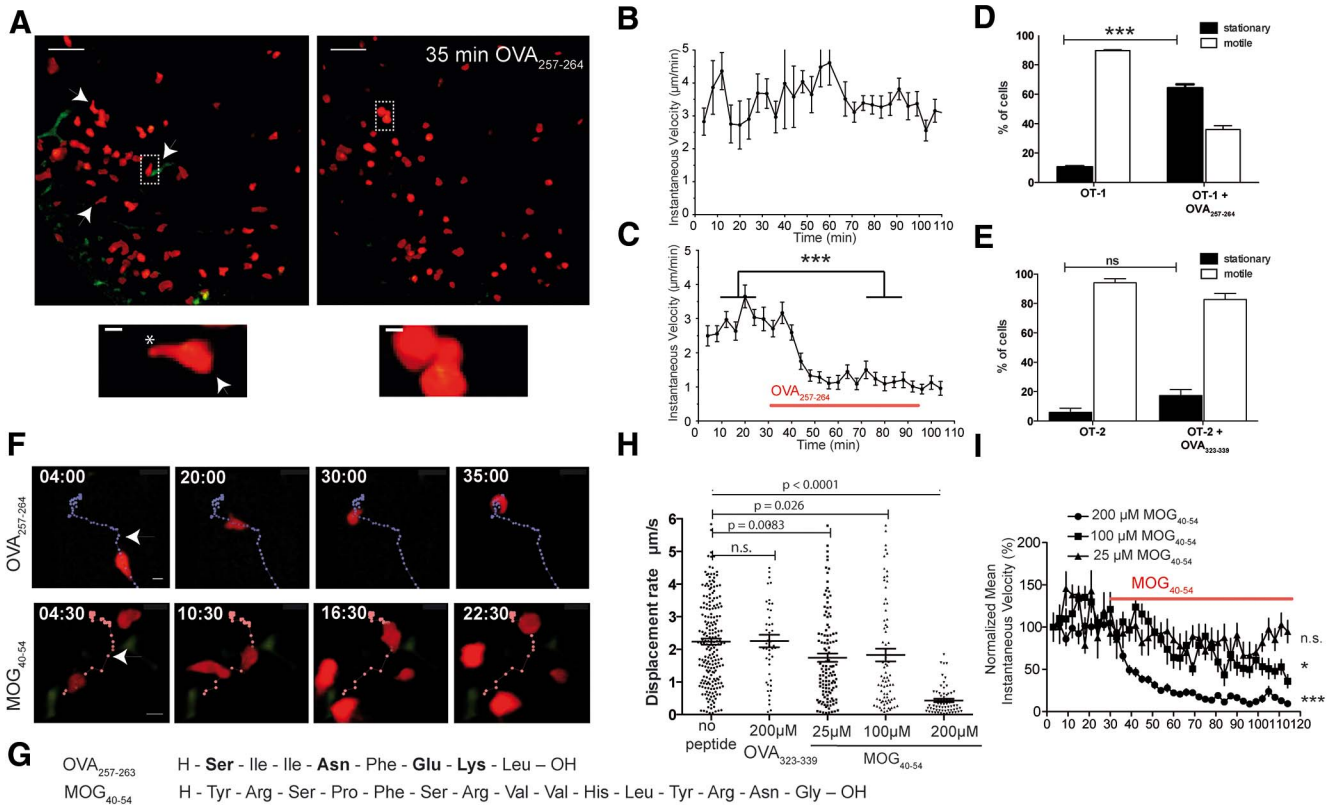

Figure 2. OT-1 CD8$^+$ T cells in organotypic brain slices. ***A***, *In vitro*-activated OT-1 CD8$^+$ T cells (left) in an acute hippocampal slice show continuous propulsive motility (scale bar, 100 μm), characterized by a round leading edge (arrowhead) and a trailing uropod (asterisk) as shown in magnification (scale bar, 10 μm). The addition of 25 nM $OVA_{257-264}$ peptide resulted in rounding and stopping of OT-1 CD8$^+$ T cells (***A***, right), a typical behavior of antigen recognizing cells. ***B***, Quantitative analysis of mean instantaneous cell velocity reveals continuously high velocity of OT-1 CD8$^+$ T cells in the absence of antigen (36 cells tracked, mean ± SEM). ***C***, After application of 25 nM $OVA_{257-264}$, instantaneous velocity of OT-1 T cells decreases strongly (Mann–Whitney-*U* test; $^{***}p < 0.0001$, 26 cells, mean ± SEM). ***D***, Static cells among OT-1 CD8$^+$ T cells show highly significant increases, from 10.3% to 69.4%, after OT-1 $OVA_{257-264}$ application (Mann–Whitney-*U* test; $^{***}p < 0.0001$, mean ± SEM). ***E***, Similar experiments with OT-2 CD4$^+$ T cells show that $OVA_{323-339}$ (CD4-OVA) application does not increase the number of stationary cells in the OT-2 CD4$^+$ T-cell hippocampal cocultures (mean ± SEM). ***F***, $OVA_{257-264}$ application leads to rounding of the formerly ovoid and propulsive OT-1 cells. Similarly, 200 μM MOG_{40-54} induces a slowing down to stationary motility. Peptides were added 10 min after starting the time-lapse acquisition (start of antigen application in respect to the depicted tracks is marked with an arrowhead; scale bar, 10 μm). ***G***, Amino acid sequence of $OVA_{257-264}$ and MOG_{40-54}. ***H***, The stopping motility (mean displacement) induced by MOG_{40-54} is concentration dependent. In contrast, the control peptide ($OVA_{323-339}$) does not induce motility changes (Kruskal–Wallis test; Dunn's post test). ***I***, Mean instantaneous velocity (± SEM) of OT-1 T cells is shown for each time point and each condition compared with before application of the substance. Concentrations of 25, 100, or 200 μM MOG_{40-54} have been compared with the baseline in the same experiment (Mann–Whitney-*U* test; $^{*}p < 0.05$, $^{***}p < 0.0001$). All data are representative of at least three experiments.

sary because the brainstem of mice and the lesion distribution and morphology is variable in between different mice.

On day 25, immune cells were isolated from the spleen and CNS of the separately cotransferred mice. In the spleen, large numbers of the transferred CD8$^+$ T cells were found (Fig. 3*C*); within the CNS, only very few of these cells were identified (Fig. 3*D*). Upon restimulation with plate-bound anti-CD3/anti-CD28 antibodies, strong IFN-γ production was recalled similarly for control and OT-1 CD8$^+$ T cells isolated from the spleen (Fig. 3*E*) or the CNS (Fig. 3*F*). Therefore, in the absence of disease induction by CD4$^+$ T cells, the cross-reactivity of a myelin antigen by CD8$^+$ T cells did not induce CNS inflammation. This indicates that only a few activated myelin-specific CD8$^+$ T cells can reach or be retained in the CNS under steady-state conditions in the absence of CD4$^+$ T cells.

Transfer of activated OT-1 T cells and pcCD8$^+$ T cells into ongoing EAE leads to selective recruitment of OT-1 T cells to inflammatory lesions

To investigate whether activated OT-1 T cells recognize their cognate antigen in established EAE lesions, we induced the disease by transfer of MOG-transgenic CD4$^+$ (2d2) Th17 cells in lymphopenic B6.RAG-1$^{-/-}$ × *thy1*.EGFP (green fluorescent axons) mice (Siffrin et al., 2010). We previously investigated CD8$^+$ T cells in active EAE, in which endogenous CD4$^+$ and CD8$^+$ T cells enter the CNS (Leuenberger et al., 2013). Based on these observations, we chose the adaptive transfer model (2d2 Th17 transfer to induce the disease) here to have a situation without endogenous CD8$^+$ T cells and thus to compare OT-1 versus pcCD8$^+$ T cells, which had clear and similar stimulation conditions.

For TPLSM, we cotransferred both OT-1 T cells (constitutively expressing tdRFP) and control polyclonally stimulated CD8$^+$ T cells (constitutively expressing CFP) into these mice, similarly as in the experiment for Figure 3*B*. The rationale for the cotransfer was to have both populations in one mouse for reasons of internal control in imaging. After transfer of both CD8 T-cell populations in EAE mice, we detected high numbers of CD8$^+$ T cells infiltrating the CNS as sign of selective enrichment of OT-1 T cells compared with pcCD8$^+$ T cells (Fig. 4*A*,*D*; Video 1). Cell tracking analysis revealed a complex motility pattern of OT-1 T cells and pcCD8$^+$ T cells in respect to the axonal compartment (Fig. 4*B*,*C*). Compared with the polyclonal CD8$^+$ T cells, OT-1 T cells exhibited a significant reduction in mean displacement rate

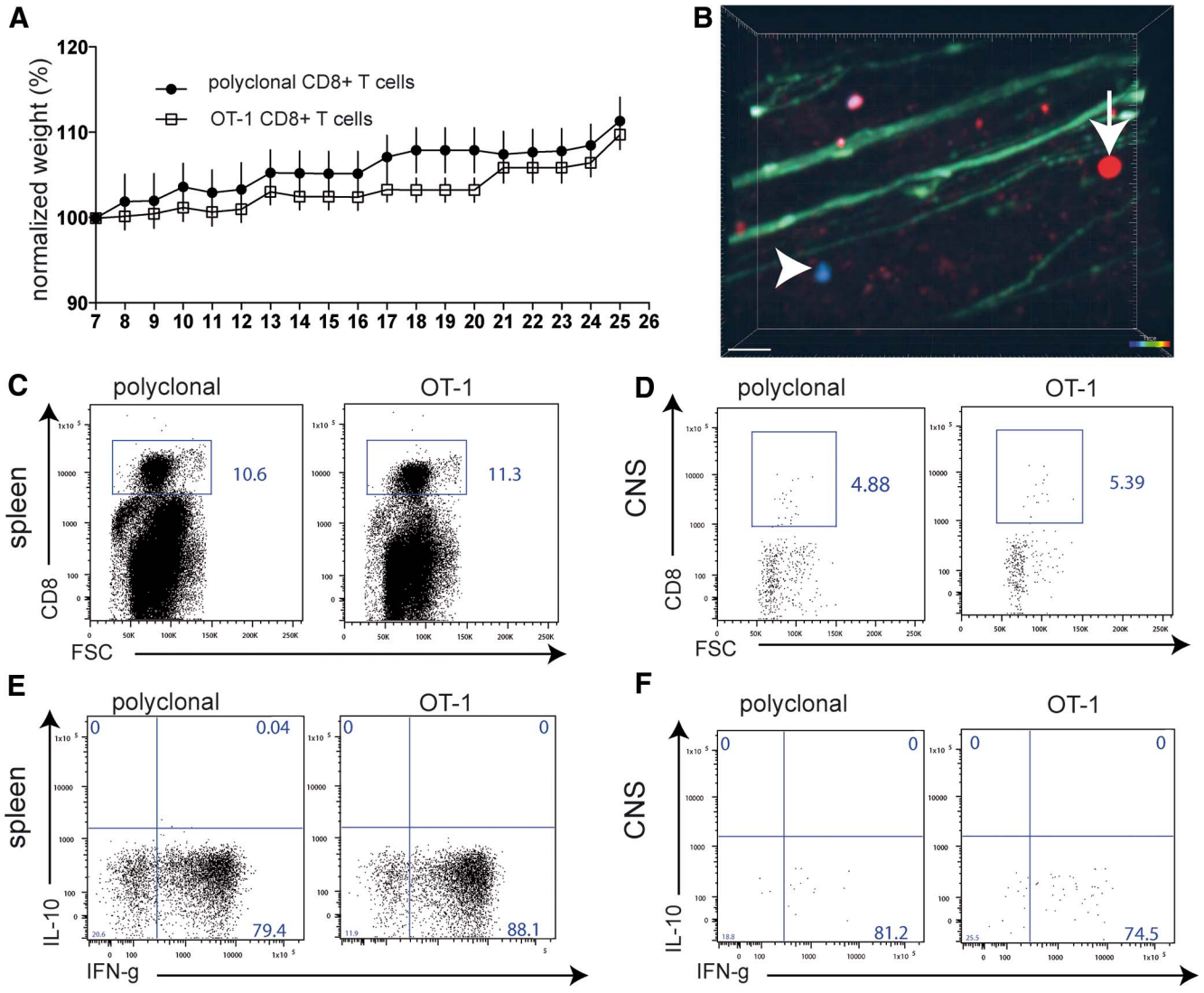

Figure 3. Transfer of activated OT-1 CD8$^+$ T cells into lymphopenic mice. OT-1 spleen cells were activated by 50 nM $OVA_{257–264}$ in the presence of IL-12 and IL-18. As the control, anti-CD3/anti-CD8 polyclonally activated wild-type C57BL/6 spleen-derived CD8$^+$ T cells were similarly activated. A total of 5×10^6 activated CD8$^+$ T cells were injected on day 7 of culture into naive lymphopenic Rag1$^{-/-}$ mice ($n = 8$, data representative of two experiments). ***A***, CD8$^+$ T-cell-transferred Rag1$^{-/-}$ mice were monitored for weight loss for 26 d and clinically evaluated according to EAE function scores. ***B***, TPLSM of the brainstem of living anesthetized Rag1$^{-/-}$/*thy1*-EGFP mice, which had been injected with red-fluorescent OT-1 cells and blue fluorescent pcCD8$^+$ T cells, showed only a few, most likely perivascular, activated OT-1 T cells and control pcCD8$^+$ T cells in the CNS without signs of CNS tissue invasion (representative of six imaging areas from two experiments; scale bar, 30 μm). ***C***, On day 25, immune cells were isolated from spleens in which large numbers of the transferred CD8$^+$ T cells could be found. ***D***, In the same animals as in ***C***, only very few cells in total and low numbers of transferred CD8$^+$ T cells (OT-1 or pcCD8$^+$ T cells) could be found by flow cytometry in CNS isolated immune cells (single dot represent single cells; pooled CNS samples from three animals). ***E***, Upon restimulation with plate-bound anti-CD3/anti-CD28 antibodies, strong IFN-γ production was recalled in the same way for both control and OT-1 CD8$^+$ T cells isolated from the spleen or the CNS (***F***).

(Fig. 4*E*), which is indicative for antigen recognition motility. We detected highly motile infiltrating T cells in areas of intact axons (Fig. 5*A*, green box; Video 2), both OT-1 T cells and, in lower numbers, polyclonal CD8$^+$ T cells (Fig. 5*B*, Video 3). T-cell tracking revealed undirected cell paths but often with regionalized migration (Fig. 5*D*, top). We identified areas of injured axons (Fig. 5*A*, red box) via focal swellings or fragmentation (Kerschensteiner et al., 2005; Siffrin et al., 2010) and observed more OT-1 T cells with directive and also stationary migratory paths, which was in clear contrast to polyclonal CD8$^+$ T cells (Fig. 5*C*,*D*, bottom). Analysis of cell motility in both CD8$^+$ T-cell groups revealed a reduced displacement rate of OT-1 CD8$^+$ T cells compared with the polyclonal CD8$^+$ T cells (Fig. 5*E*) and also between OT-1 T cells near damaged axons and OT-1 T cells near intact axons. This indicates that cross-recognition takes place under inflammatory conditions and is more pronounced in more severe lesions. Statistical analysis of the track motility pattern was performed as described previously with slight adaptations to our system [stopping cells (<3 μm/min), swarming/kinapse cells (≥ 3 μm/min <6 μm/min), and nonrestricted cell movement (>6 μm/min)]. This analysis confirmed the observation that antigen recognition was found mainly in OT-1 T cells and rarely in pcCD8$^+$ T cells (Fig. 5*F*). In addition, areas with injured axons had higher numbers of stopping and swarming OT-1 T cells than areas with morphologically intact axons, which might correlate with the presence of disrupted myelin. However, direct interactions with axons could not be confirmed (Fig. 6*A*,*B*), in contrast to CD4$^+$ T-cell interactions with axons (Fig. 6*C*,*D*, red, 2d2 Th17 cells; Video 4), which we have described previously in detail (Siffrin et al., 2010).

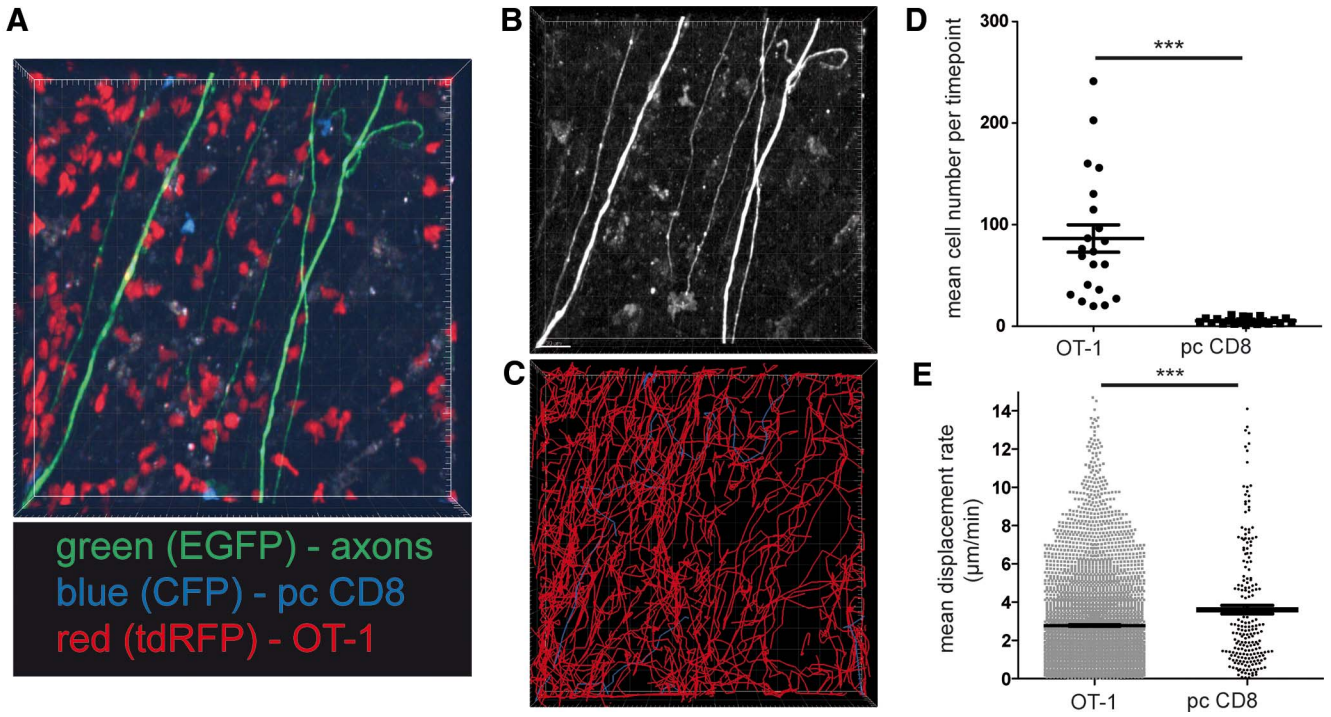

Figure 4. Transfer of activated OT-1 T cells into ongoing EAE. EAE was induced in Rag1 $^{-/-}$/*thy1*-EGFP mice (green fluorescent axons) by transfer of MOG_{35-55} TCR transgenic 2d2 CD4 $^{+}$ Th17 cells. Both OT-1 CD8 $^{+}$ T cells and control polyclonal (pc) CD8 $^{+}$ T cells were cotransferred 7 d after 2d2 transfer. OT-1 T cells (constitutively expressing tdRFP) and control pcCD8 $^{+}$ T cells (constitutively expressing CFP) had been activated in the presence of IL-12 and IL-18. For TPLSM, both CD8 $^{+}$ T-cell subsets were cotransferred together in recipient animals ($n = 18$, data representative of six experiments). ***A***, CNS-infiltrating cells revealed red OT-1 cells and blue CFP cells with more OT-1 than pcCD8 (imaging area: 300 × 300 × 70 μm). ***B***, High-contrast depiction of EGFP fluorescent structures (axons). ***C***, Display of individual cell tracks (OT-1 in red, pcCD8 $^{+}$ in blue) of the recording as shown in ***A*** reveals complex motility pattern of OT-1 and pcCD8 $^{+}$ in EAE lesions (observation time 45 min). ***D***, Mean cell numbers per time point of OT-1 or pcCD8 $^{+}$ T cells were analyzed for 12 time-lapse recordings from 18 recordings of six experiments. OT-1 cells strongly outnumbered pcCD8 $^{+}$ T cells in EAE lesions; Mann–Whitney-*U* test was performed; ***$p < 0.0001$. ***E***, Mean displacement rate of OT-1 or pcCD8 $^{+}$ T cells from cell tracking analysis as shown in ***D*** are displayed. OT-1 have a lower displacement rate than pcCD8 $^{+}$, which indicates a higher number of antigen recognizing CD8 $^{+}$ T cells in the OT-1 population (Mann–Whitney-*U* test; ***$p <$ 0.0001).

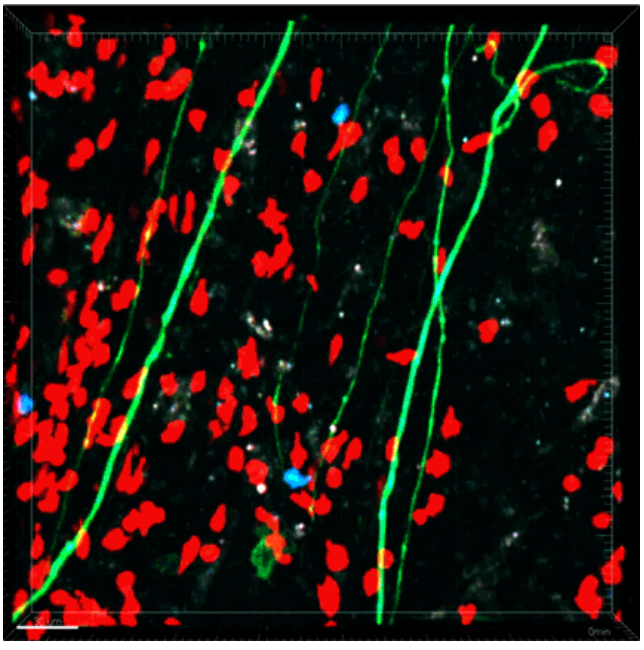

Video 1. Intravital imaging of living anesthetized CD4-induced EAE (nonfluorescent 2d2 Th17 cells for induction) in RAG1 $^{-/-}$ × *thy1*-EGFP mouse (axons in green) that had been transferred with OT-1 (red) and pcCD8 $^{+}$ T cells (CFP).

MOG_{40-54} reactive OT-1 T cells do not induce clinical or subclinical damage in EAE lesions despite antigen recognition motility

Next, we investigated the association of CD8 $^{+}$ (MOG-recognizing; Fig. 7*A*, Video 5) and CD4 $^{+}$ T cells (MOG-recognizing; Fig. 7*B*, Video 6) with intra-axonal Ca^{2+} increase, which is the earliest sign of axonal damage even before morphologic changes. We used mice that express a genetically encoded Ca^{2+} sensor in neurons and axons (*thy1*-TN-XXL; Mank et al., 2008) in a similar experimental approach as that for the *thy1*-EGFP mice. Here, we could confirm that the specific interactions of CD8 $^{+}$ T cells with axons were rather subtle (Fig. 7*C*), whereas the CD4 $^{+}$ T cells often enwrapped the whole axon for a prolonged period of time (Fig. 7*D*). On the functional level, the latter form of contact was associated with higher intra-axonal Ca^{2+} levels in the axons in contact with CD4 $^{+}$ T cell (Fig. 7*E*) than those in contact with CD8 $^{+}$ T cells (Fig. 7*F*).

To change the focus from intravital imaging to clinical evaluation of CD8-mediated damage processes, we switched from passive to active EAE, which usually leads to a less severe disease course and therefore allows longer monitoring. We cotransferred activated OT-1 CD8 $^{+}$ T cells on day 7 after active EAE induction (Fig. 8*A*). Control mice received polyclonally activated wild-type CD8 $^{+}$ T cells on day 7. The positive control was a group of mice that received 2d2 Th17 cells, which induces a neurodegenerative phenotype when transferred into active EAE (Siffrin et al., 2010); the negative control group received a saline injection. The severity of clinical signs did not differ between the CD8 $^{+}$ transferred

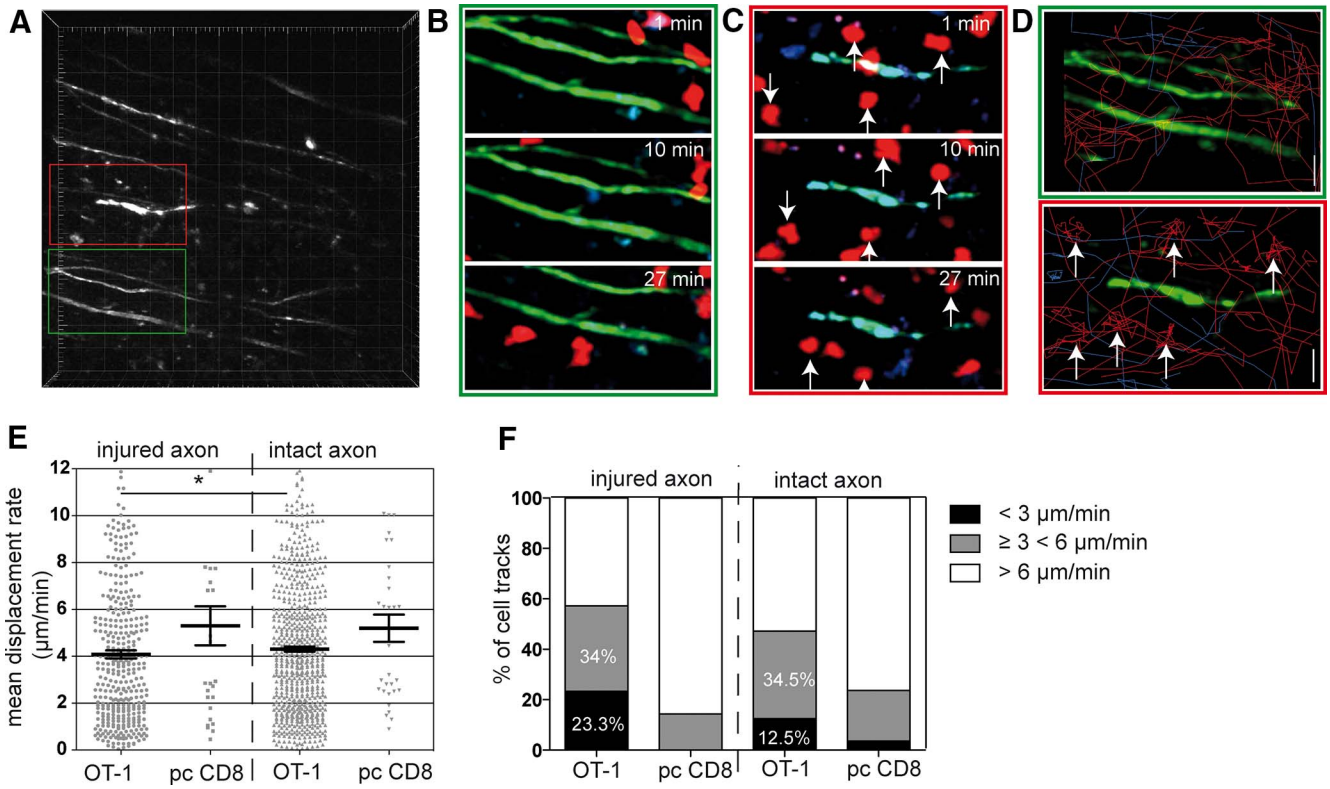

Figure 5. Analysis of CD8 $^+$ T-cell motility in relation to axonal injury. In the recordings, as shown in Figure 4, the interaction between OT1 or polyclonal CD8 $^+$ T cells with axons was analyzed. Some axons show typical signs of damage (swellings, fragmentation, ellipsoid bodies) due to EAE pathology; others were morphologically intact. Image areas with damaged axons (red boxed area) were compared with areas without damage (green boxed area). ***A***, Overview high-contrast depiction of EGFP fluorescence (axons), two relevant sections are enlarged to highlight areas of axonal integrity (green frame) and axonal injury (red frame), which are found close to each other. Injured axons are characterized by focal swelling and an irregular shape of axon cross section. ***B***, In areas of intact axons (green frame in ***A***), both OT-1 and pcCD8 $^+$ T cells exhibit propulsive motility/morphology. ***C***, In areas of injured axons (red frame in ***A***), OT-1 T cells show rounding as a sign of stopping. ***D***, Depiction of individual cell paths (OT-1: red, pcCD8 $^+$: blue) in area of intact (top) versus injured (bottom) axon(s). ***E***, Analysis of several recordings similar to ***A*** reveals a decrease in mean displacement rate in areas of injured axons compared with intact areas (18 individual recording from six experiments, Mann–Whitney-*U* test; $*p = 0.025$). ***F***, Analysis of mean velocity and stratification of cell tracks with stationary motility (<3 μm/min), swarming motility (≥ 3 and <6 μm/min), and random migration velocity (>6 μm/min) from 18 individual recordings from six experiments. The percentage of cells with the respective motility pattern is shown.

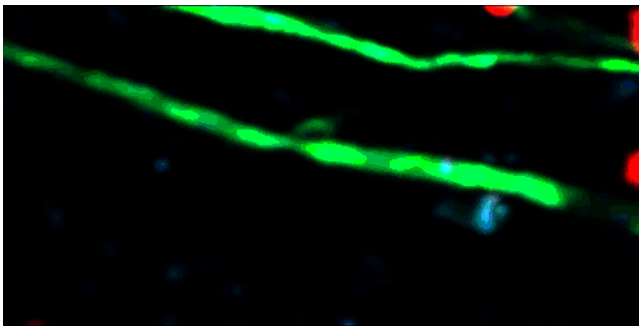

Video 2. Intravital imaging of living anesthetized CD4-induced EAE (nonfluorescent 2d2 Th17 cells for induction) RAG1 $^{-/-}$ × *thy1*-EGFP mouse (axons in green) that had been transferred with OT-1 (red) and pcCD8 $^+$ T cells (CFP). OT-1 T-cell migration can be seen near intact axons.

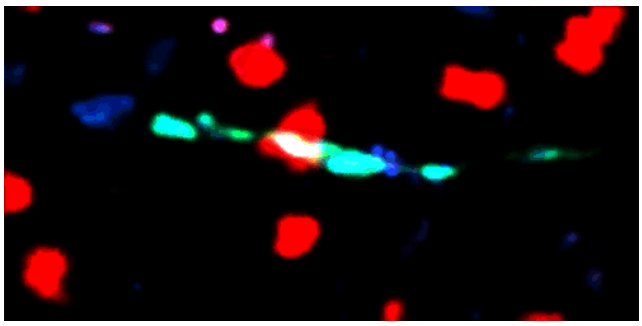

Video 3. Intravital imaging of living anesthetized CD4-induced EAE (nonfluorescent 2d2 Th17 cells for induction) RAG1 $^{-/-}$ × *thy1*-EGFP mouse (axons in green) that had been transferred with OT-1 (red) and pcCD8 $^+$ T cells (CFP). OT-1 T-cell migration can be seen in respect to injured axons.

groups (activated OT-1 or polyclonal CD8 $^+$ T cells), whereas the 2d2 Th17 transferred mice underwent a more severe disease course. Both CD8 $^+$ T-cell subsets showed a strong activation phenotype before transfer (Fig. 8*B*) and we identified a significant number of the transferred CD8 $^+$ T cells. Upon re-isolation of T cells from mice that had received both CD8 $^+$ T-cell subsets (OT-1 plus pcCD8 $^+$ T cells), we were able to detect OT-1 T cells and pcCD8 $^+$ T cells in the spleen and CNS. Consistent with the findings from the TPLSM results of the adoptive transfer EAE model described above, OT-1 T cells were enriched in the CNS. More OT-1 T cells were recruited than pcCD8 $^+$ T cells compared with reference ratios from the spleens (Fig. 8*C*,*D*). In addition, in the CNS, there were significantly more IFN-γ producers among OT-1 T cells than among the polyclonal CD8 $^+$ T cells (Fig. 8*E*), indicating once more either selective enrichment of these strongly activated OT-1 T cells or local reactivation. To evaluate subclinical damage processes in the context of either OT-1 or pcCD8 $^+$ T cells, we performed standard histology from animals

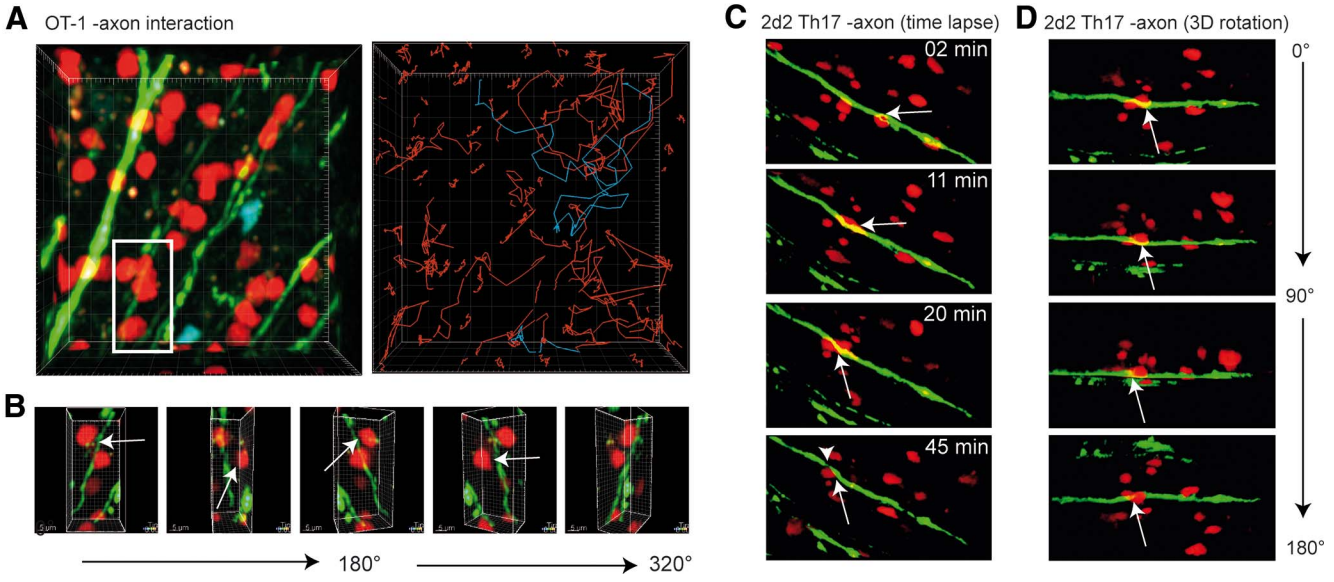

Figure 6. Analysis of interactivity of T cells with axons. EAE was induced in Rag1 $^{-/-}$/*thy1*-EGFP mice (green fluorescent axons) by transfer of MOG_{35-55} TCR-transgenic 2d2 CD4 $^{+}$ Th17 cells. Both OT-1.tdRFP CD8 $^{+}$ T cells and control polyclonal (pc) CD8 $^{+}$ T cells (CFP) were cotransferred 7 d after 2d2 transfer. ***A***, Area of axonal injury with numerous OT-1 T cells (red), which exhibit stationary motility; pcCD8 $^{+}$ T cells with free migration. Right, Analysis of cell tracks (OT-1: red, pcCD8 $^{+}$: blue). ***B***, 360° rotation along the *y*-axis of the boxed area (white) in ***A***. Arrows indicate the distance between axons and OT-1 C8+ T cells. ***C***, EAE was induced in Rag1 $^{-/-}$/*thy1*-EGFP mice (green fluorescent axons) by transfer of red-fluorescent MOG_{35-55} TCR-transgenic 2d2.tdRFP CD4 $^{+}$ Th17 cells. 2d2.tdRFP Th17 cells (red, arrow) interact with axons. Axon exhibits thinning after interaction with 2d2 Th17 cell as sign of imminent dissection (arrowhead). ***D***, Rotation along a horizontal axis of image area in ***C*** shows close proximity of axons and 2d2.tdRFP Th17 cell (arrow).

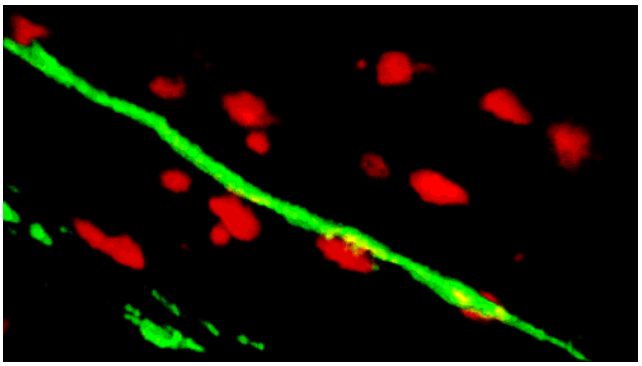

Video 4. Intravital imaging of living anesthetized RAG1 $^{-/-}$ × *thy1*-EGFP mouse (axons in green) mouse that had been induced for EAE by red-fluorescent 2d2 Th17 CD4 $^{+}$ T cells (red). CD4 $^{+}$ T-cell interaction with axon can be seen.

that were killed on day 22 (14 d after CD8 $^{+}$ T-cell transfer). Histopathological semiquantitative analysis revealed that the characteristics of invading immune cells were similar in both groups (Fig. 9*A*,*B*). The extent of demyelination was analyzed by semiquantitative evaluation of MBP loss in white-matter tracts, which showed no differences between the groups (Fig. 9*C*). In addition, the extent of axonal damage was comparable between the two groups, as identified by similar loss of neurofilament-positive neurons/axons in demyelinated lesions (Fig. 9*D*). Therefore, we did not find any differences in damage either to myelin sheaths or to axons/neurons in EAE lesions, although strongly activated and enriched OT-1 T cells were found in high numbers. In summary, we showed that there is specific recognition of MOG_{40-54} by OVA-transgenic (OT-1) CD8 $^{+}$ T cells in the CNS *in vivo* but that this was not sufficient to induce either clinically or subclinically detectable CNS damage.

Discussion

The role of CD8 $^{+}$ T cells in the pathology of multiple sclerosis has been the subject of controversy for many years (Neumann et al., 2002; Siffrin et al., 2007; Friese and Fugger, 2009). We made use of this model of myelin-recognizing transgenic CD8 $^{+}$ T cells to analyze the intriguing model of molecular mimicry for the first time in EAE lesions *in vivo* by TPLSM. Myelin cross-reactive OT-1 T cells exhibited characteristic antigen-recognition motility changes in areas of axonal injury without the need for exogenous antigen application. Therefore, these cross-reactive, highly activated CD8 $^{+}$ T cells were markedly enriched in the CNS, but only in established EAE lesions. Nevertheless, these myelin-recognizing, activated CD8 $^{+}$ T cells did not result in CNS damage within the CNS under *in vivo* conditions; that is, in naive lymphopenic mice or in ongoing autoimmune CNS inflammation in EAE mice.

The strongest arguments in support of an active role of CD8 $^{+}$ T cells in the pathology of autoimmune neuroinflammation have been derived from studies of the human disease, which describe the presence of CD8 $^{+}$ T cells in multiple sclerosis lesions (Babbe et al., 2000; Kim et al., 2012; Siewert et al., 2012). These reports have fueled many approaches for finding animal models of CD8-mediated neuroinflammation. However, genuine CD8-induced EAE models are much rarer than CD4-mediated EAE models, which come in many different forms (Krishnamoorthy and Wekerle, 2009). Whereas the relevance of CD4 $^{+}$ T cells, in particular for autoimmune demyelinating neuroinflammation (Petermann and Korn, 2011), is undeniable, the contribution of CD8 $^{+}$ T cells to CNS damage is much more controversial. There have been two studies showing a clear disease-inducing role of CD8 $^{+}$ T cells by transfer of myelin-specific CD8 $^{+}$ T cells (Huseby et al., 2001; Sun et al., 2001). In contrast, the majority of studies emphasize very mild, EAE-uncharacteristic or even absent clinical deficits compared with the CD4 $^{+}$ T-cell-mediated disease (Ford and Evavold, 2005; Friese et al., 2008; Saxena et al., 2008; Ji et al., 2010; Ander-

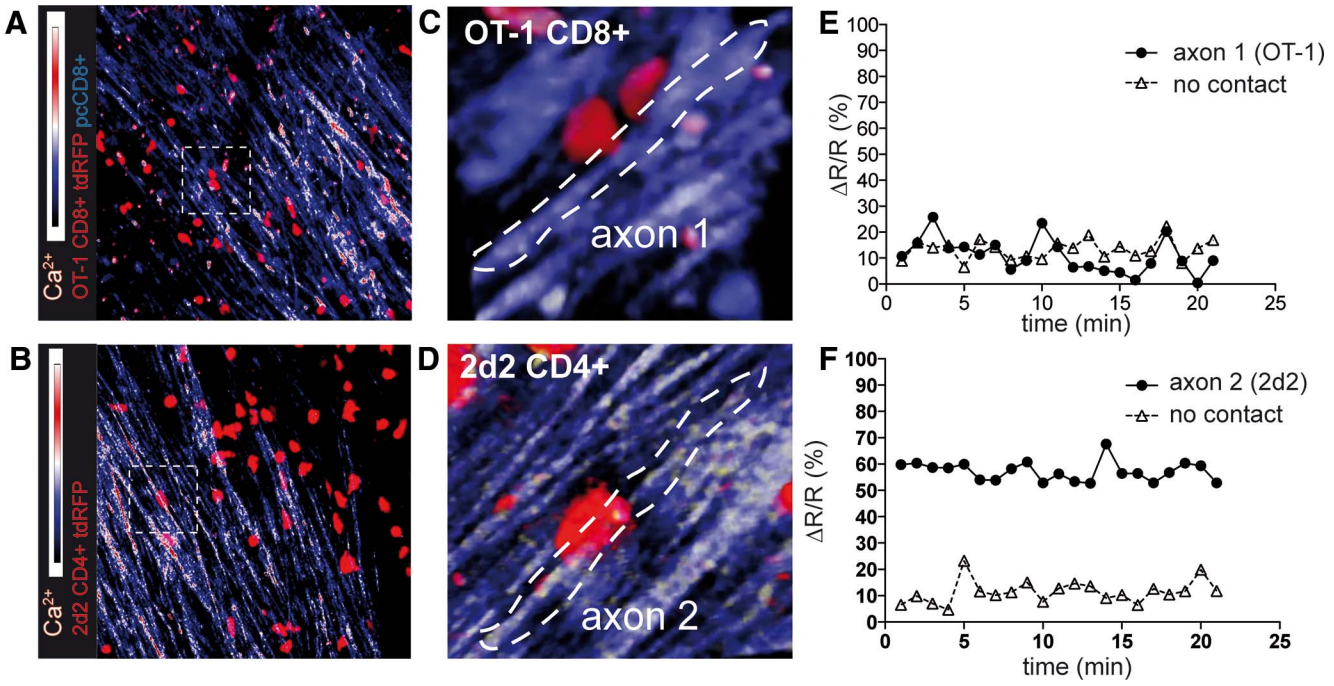

Figure 7. *In vivo* intra-axonal Ca^{2+} evaluation to quantify axonal injury in relation to T-cell interactions. EAE was induced in Rag1 $^{-/-}$/thy1-TN-XXL mice (genetically encoded troponin-C based Ca^{2+} sensor) by transfer of MOG_{35-55} TCR transgenic nonfluorescent 2d2 $CD4^+$ Th17 cells (***A***, ***C***) or red fluorescent 2d2.tdRFP Th17 cells (***B***, ***D***). Ca^{2+} levels are shown as the YFP/CFP ratio; data representative of at least three independent experiments. ***A***, Activated, red-fluorescent OT-1.tdRFP $CD8^+$ T cells and control polyclonal (pc.EGFP) $CD8^+$ T cells were cotransferred 7 d after 2d2 transfer. As in Figures 4 and 5, interactions of $CD8^+$ T cells were visualized. Intra-axonal Ca^{2+} is shown as the ratio channel (heat map: blue-red). Only few axon-associated OT-1.tdRFP cells were associated with increased intra-axonal Ca^{2+} levels. ***B***, Disease-inducing 2d2.tdRFP Th17 cells strongly associated with high Ca^{2+} axons. ***C***, 3D time-lapse imaging of the boxed area in ***A*** is shown and reveals the subtle contact formation (arrowhead) of static OT-1.tdRFP cells with axons (CFP channel: blue, YFP channel: yellow). ***D***, 3D time-lapse imaging of the boxed area in ***B*** is shown and reveals the strong contact formation (arrowhead) of the 2d2.tdRFP cell with an axon that is tightly enwrapped by the T lymphocyte. ***E***, 2d2.tdRFP $CD4^+$ T cell (arrow in ***D***) contacted axon. Mean relative Ca^{2+} levels in contacted axon 1 compared with control axon with no T-cell contact in the same recording. ***F***, OT-1.tdRFP $CD8^+$ T-cell-contacted axon 2 (arrow in ***C***). Mean relative Ca^{2+} levels in the contacted axon compared with a control axon with no T-cell contact in the same recording.

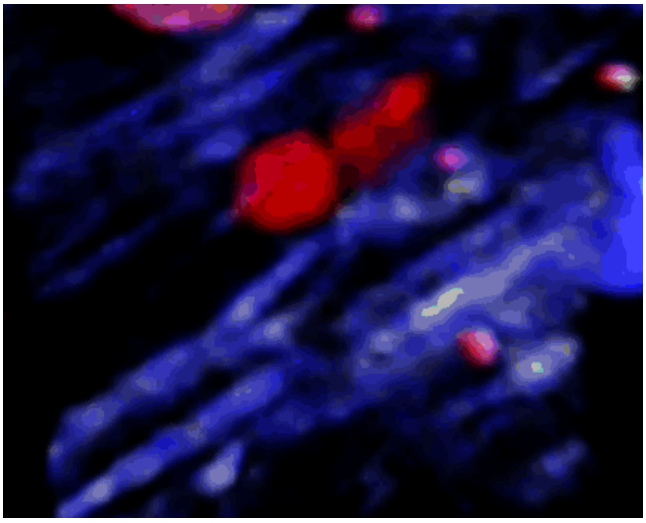

Video 5. Intravital imaging of living anesthetized CD4-induced EAE (nonfluorescent 2d2 Th17 cells for induction) RAG1 $^{-/-}$ × *thy1*-TN-XXL mouse (axons in blue, Ca^{2+} yellow-white) that had been transferred with OT-1 (red) and pcCD8 $^+$ T cells (blue). OT-1 T-cell motility can be seen in respect to injured axons.

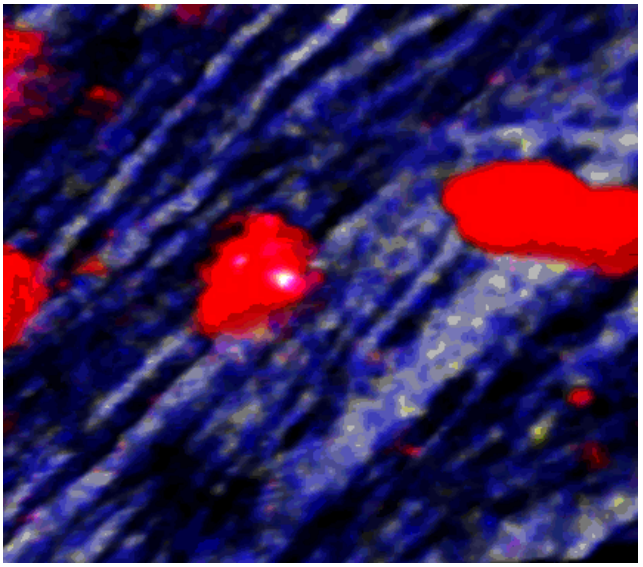

Video 6. Intravital imaging of living anesthetized RAG1 $^{-/-}$ × *thy1*-TN-XXL mouse (axons in blue, Ca^{2+} yellow-white) mouse that had been induced for EAE by red-fluorescent 2d2 Th17 $CD4^+$ T cells (red). $CD4^+$ T-cell interaction with axon can be seen.

son et al., 2012; Na et al., 2012). In addition, in most of these CD8 models, the assistance of $CD4^+$ T cells seems to be essential for full-blown autoimmune neuroinflammation (Leuenberger et al., 2013).

The basic requirements for specific antigen recognition of $CD8^+$ T cells is presentation by MHC-I molecules (Townsend et al., 1989). In this study, using intravital imaging, we discovered that, in principle, OT-1 T cells are able to recognize both their

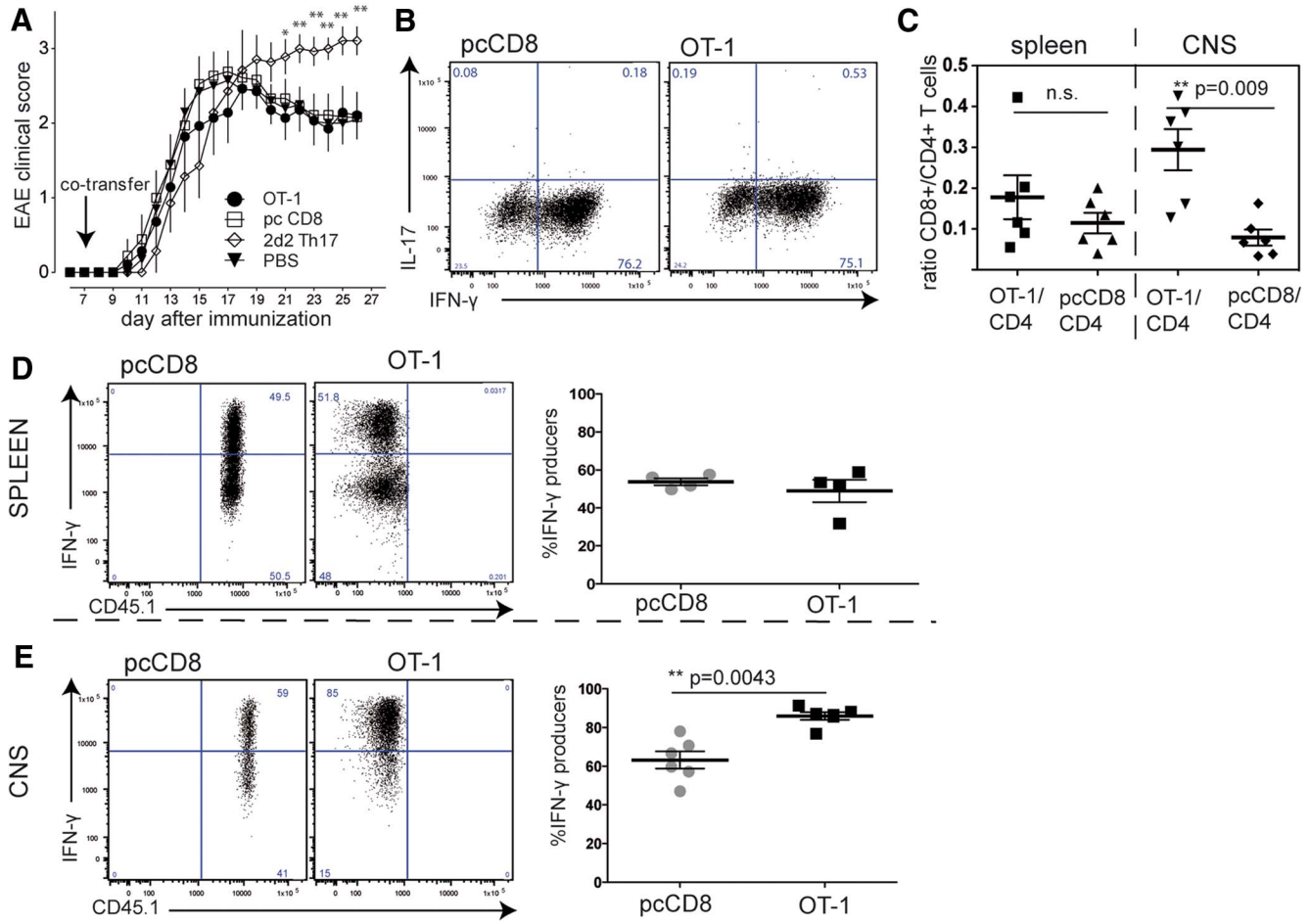

Figure 8. Evaluation of EAE upon OT-1 T-cell transfer. EAE was induced in C57BL/6 mice by subcutaneous immunization with CFA/$MOG_{35–55}$. A total of 30×10^6 activated $CD8^+$ T cells were cotransferred on day 7 after EAE induction. ***A***, Mean clinical score of OT-1-cotransferred, $pcCD8^+$ T-cell-transferred, or PBS-injected mice were evaluated. There was no significant difference between the $CD8^+$ T-cell-transferred groups and the PBS control; 2d2 Th17 induced disease exacerbation compared with PBS control and to $CD8^+$ T-cell-transferred mice ($n = 7$, statistical analysis of each cell-transferred group vs PBS control by Mann–Whitney-*U* test; $*p < 0.05$, $**p < 0.01$). ***B***, Cytokine expression profile of OT-1 and $pcCD8^+$ T cells on the day of transfer into recipient animals reveals strong and comparable activation of both $CD8^+$ T-cell populations. ***C***, For analysis of selective enrichment, mice received both OT-1 and $pcCD8^+$ T cells analogously to the experiments shown in Figures 4 and 5. The ratio of OT-1/$CD4^+$ T cells was increased in the CNS compared with $pcCD8^+/CD4^+$ T cells within the CNS. These ratios were similar in the spleen. The Mann–Whitney-*U* test was performed. ***D***, Spleen-isolated OT-1 T cells and polyclonal control $CD8^+$ T cells exhibited comparable amounts of IFN-γ producers after *in vitro* CD3/28 restimulation. ***E***, CNS-isolated OT-1 T cells were significantly more numerous IFN-γ producers than the $pcCD8^+$ T cells.

(high-affinity) cognate and a (medium-affinity) myelin antigen in the CNS. $CD8^+$ T-cell antigen recognition of $MOG_{40–54}$ could be shown by three independent conventional readouts: T-cell proliferation, cytotoxic activity, and binding of peptide–MHC-I tetramers. These are three fundamentally different events that follow the T-cell–APC interaction. Proliferation—similarly to cytokine production—is a postnuclear response that necessitates active transcription events. Cytotoxicity is a prenuclear event that involves the release of preformed vesicles with cytotoxic substances. Tetramer staining shows the binding of the specific peptide MHC-I to the TCR. In our slice experiments, this TCR-MHC/myelin antigen binding resulted in strong changes of migratory activity in T cells; for example, immobilization (stop signal) following antigen recognition, which is consistent with reports using other models (Shakhar et al., 2005). This stopping motility has been correlated with subsequent cell proliferation, effector cytokine production, and cytotoxic activity. In contrast, inefficient TCR-MHC/antigen binding does not induce major motility changes *in vivo* (Skokos et al., 2007) and instead results in T-cell tolerance (Marangoni et al., 2013). Application of these basic rules of T-cell activation motility highlights the fact that there is sufficient MHC-I/peptide expression in EAE lesions in our experiments.

OT-1 T cells exhibited full activation motility *in vivo*, predominantly in areas of strong axono–glial injury. However, this cross-reactivity neither increased histological nor intravital signs of damage nor clinical signs of damage such as weight loss or EAE symptoms, indicating that $CD8^+$ T cells are not the main inducers of damage. Direct observation of the lesions *in vivo* by TPLSM showed an induction of sustained Ca^{2+} increase in axons that were attacked by 2d2 $CD4^+$ Th17 cells, but not in axons that were surrounded by stopping OT-1 $CD8^+$ T cells. Despite these observations, which refute a direct interaction of $CD8^+$ T cells with axons and also an effect of stopping OT-1 T cells on nearby axons, we cannot completely exclude a cell-contact-independent effect, although neither microscopy nor histology nor clinical data support damage induction by cross-reactive OT-1 T cells.

It is difficult to reconcile the finding of full reactivation of cross-reactive $CD8^+$ T cells in the CNS *in vivo*, as we have described it here, with the absence of cytotoxicity toward the axono–glial unit. It is rather unlikely that the activation of T cells in

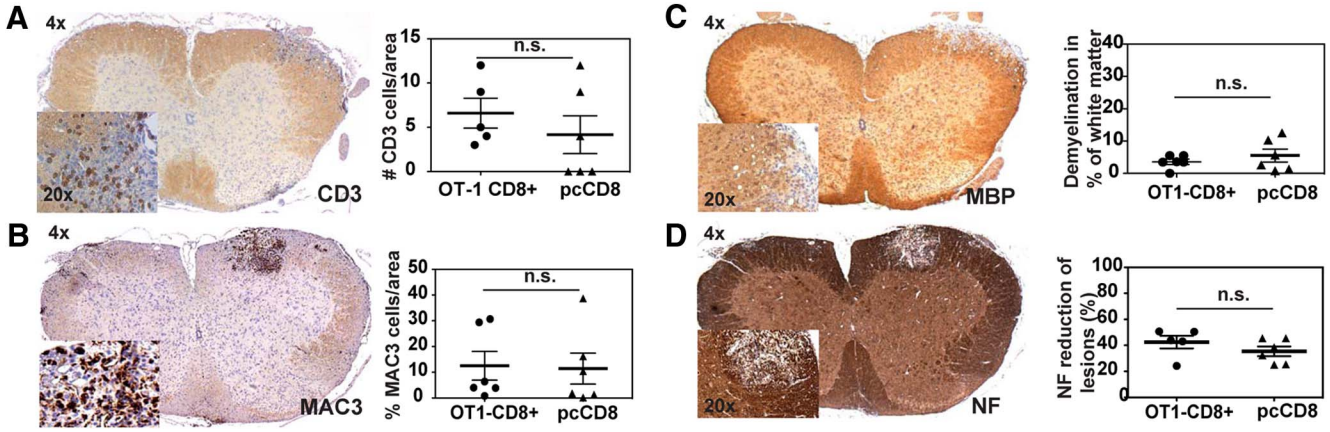

Figure 9. Histopathological semiquantitative analysis of spinal cord tissue. Standard histopathology was performed on paraffin-embedded tissue samples of animals that had been killed on day 22 after EAE induction (14 d after CD8$^+$ T-cell cotransfer). Shown are the pooled data of two independent experiments ($n = 10$/experiment). ***A***, CNS-infiltrating CD3 cells are similarly distributed in both groups (representative slide of evaluation). Quantification of CD3 cells shows no significant differences between the OT-1 transferred and the pcCD8$^+$ T-cell-transferred groups. Each data spot represents the mean cell count per 0.01 mm^2 of individual mice. ***B***, Mononuclear phagocytic inflammatory cells (MAC-3 positive) are comparable in distribution and number in mice that were transferred with OT-1 T cells or polyclonal CD8$^+$ T cells. Each data spot represents the mean cell count per 0.01 μm^2 of individual mice. ***C***, Demyelination was similar in both groups, as analyzed by semiquantitative evaluation of MBP loss in white matter tracts (percentage of demyelinated area of all white matter area). Each data point represents the mean of an individual mouse. ***D***, Axonal loss in EAE lesions was evenly distributed between the two groups, as identified by a similar loss of neurofilament-positive neurons/axons in demyelinated lesions. Each data point represents the mean of an individual mouse. Mann–Whitney-*U* test was performed for all statistical analyses.

the CNS is too weak because immobilization—full activation in areas of destructive EAE lesions—is clearly visible in the strongly neurodegenerative lesions. However, our imaging experiments showed a lack of direct interactivity of the myelin-recognizing OT-1 T cells with axons and low association with intra-axonal Ca^{2+} increase. Therefore, a buffering of cytotoxicity by other CNS cells, for example, astrocytes, microglia, or macrophages, may explain this finding (Sun and Wekerle, 1986). In autoimmunity, these cells may indeed express higher numbers of MHC-I than neurons and oligodendrocytes.

Another explanation for the lack of cytotoxicity *in vivo* could be that the requirements for proliferation and the formation of the cytotoxic synapses are different. It has been shown that "weak agonists" induced strong proliferation (Cemerski et al., 2007) although they did not form the central supramolecular activation cluster (cSMAC). The cSMAC is the key feature of a mature immune synapse and it has been shown to be essential for cytotoxicity (Somersalo et al., 2004). Anchoring of the microtubule organizing center is strongly dependent on the presence of a stable LFA-1 supramolecular cluster that is the backbone for the lytic granule secretion machinery (Kuhn and Poenie, 2002). Therefore, we cannot support a direct role of CD8$^+$ T cells, which recognize a cross-reactive self-peptide in the CNS *in vivo*, in axon damage, in contrast to what has been described previously for CD4$^+$ T cells (Siffrin et al., 2010) amd shown here for Th17 cells and axons and elsewhere for macrophages and axons (Nikić et al., 2011). Therefore, we think that it is highly unlikely that cytotoxic T lymphocytes (CTLs) indirectly induce axonal damage in our OT-1–myelin cross-recognizing model. We cannot exclude that, of course, for other CTLs.

This opens up the question of what the basic requirements for CD8-induced damage in the CNS in the context of medium-affinity self-antigens may be. Interestingly, profound tolerance of MBP-specific CD8$^+$ TCR-transgenic mice has been described, which relied on the active removal of MHC-I/peptide complexes by high-avidity transgenic CD8$^+$ T cells without inducing proliferation or disease (Perchellet et al., 2004). In our work, similar mechanisms were not applicable. We did not find anergy of CNS-infiltrating, myelin-recognizing CD8$^+$ T cells, because the cross-reacting transgenic CD8$^+$ T cells in the CNS showed even higher IFN-γ production capacity than the polyclonal control cells. Several studies have emphasized the potential role of infectious stimuli in rendering CD8$^+$ T cells autoreactive in the CNS. Only strong activation of APC, for example, via viral infection with the *Vaccinia* virus, has been shown to break the tolerance of CD8$^+$ T cells and induce CNS autoimmune disease, which was less reminiscent of demyelinating disease and more of encephalitis (Ji et al., 2010). Another study found that ovalbumin-specific CD8$^+$ T cells failed to induce disease in animals with OVA expression in oligodendrocytes (Na et al., 2012). Only in the context of intracerebral *Listeria* infection were CD8$^+$ T cells rendered cytotoxic toward OVA-expressing oligodendrocytes. This indicates that strong costimulation in addition to TCR signaling is needed for sufficient CD8$^+$ T-cell activation. The need for strong infectious mediators (*Vaccinia*, *Listeria*) underlines the well known role of CD8$^+$ T cells, particularly in the presence of infection of the CNS. However, this is different from the situation in EAE and multiple sclerosis, where there are no strong proinflammatory infectious stimuli (e.g., pathogens in the CNS).

In the autoimmune context, which by definition has no direct causative pathogen, the model of molecular mimicry has been textbook knowledge for many years. Here, we demonstrated *in vivo* in the model disease that CD8$^+$ T-cell cross-reactivity is indeed observable in CNS lesions and leads to a selective enrichment of these cells in the CNS. This might explain the presence of oligoclonal CD8$^+$ T cells within lesions of multiple sclerosis patients (Jacobsen et al., 2002). However, that is not sufficient for a disease-modifying effect.

The question remains of how damage processes in EAE lesions are triggered if cross-reactivity of CD8$^+$ T cells alone is not sufficient. One suggestion here, supported by experimental but also recent genetic data, is that the CD4$^+$ T cell is also the relevant subset in the context of direct target organ damage (Nylander and Hafler, 2012). Considered together, CD8$^+$ T-cell-based molecular mimicry of a foreign antigen and a cross-reactive myelin an-

tigen is not sufficient for inducing axono–glial damage *in vivo*. However, it does explain the presence and enrichment of oligoclonal and CNS-specific CD8$^+$ T cells in EAE. In the end, molecular mimicry on its own is not a plausible cause of either EAE or potentially multiple sclerosis in the context of CD8$^+$ T cells in the brain.

References

Anderson AC, Chandwaskar R, Lee DH, Sullivan JM, Solomon A, Rodriguez-Manzanet R, Greve B, Sobel RA, Kuchroo VK (2012) A transgenic model of central nervous system autoimmunity mediated by CD4$^+$ and CD8$^+$ T and B cells. J Immunol 188:2084–2092. CrossRef Medline

Babbe H, Roers A, Waisman A, Lassmann H, Goebels N, Hohlfeld R, Friese M, Schröder R, Deckert M, Schmidt S, Ravid R, Rajewsky K (2000) Clonal expansions of CD8(+) T cells dominate the T cell infiltrate in active multiple sclerosis lesions as shown by micromanipulation and single cell polymerase chain reaction. J Exp Med 192:393–404. CrossRef Medline

Benoist C, Mathis D (2001) Autoimmunity provoked by infection: how good is the case for T cell epitope mimicry? Nat Immunol 2:797–801. CrossRef Medline

Bettelli E, Pagany M, Weiner HL, Linington C, Sobel RA, Kuchroo VK (2003) Myelin oligodendrocyte glycoprotein-specific T cell receptor transgenic mice develop spontaneous autoimmune optic neuritis. J Exp Med 197:1073–1081. CrossRef Medline

Celli S, Lemaître F, Bousso P (2007) Real-time manipulation of T cell-dendritic cell interactions in vivo reveals the importance of prolonged contacts for CD4$^+$ T cell activation. Immunity 27:625–634. CrossRef Medline

Cemerski S, Das J, Locasale J, Arnold P, Giurisato E, Markiewicz MA, Fremont D, Allen PM, Chakraborty AK, Shaw AS (2007) The stimulatory potency of T cell antigens is influenced by the formation of the immunological synapse. Immunity 26:345–355. CrossRef Medline

Clements CS, Reid HH, Beddoe T, Tynan FE, Perugini MA, Johns TG, Bernard CC, Rossjohn J (2003) The crystal structure of myelin oligodendrocyte glycoprotein, a key autoantigen in multiple sclerosis. Proc Natl Acad Sci U S A 100:11059–11064. CrossRef Medline

Cusick MF, Libbey JE, Fujinami RS (2013) Multiple sclerosis: autoimmunity and viruses. Curr Opin Rheumatol 25:496–501. CrossRef Medline

Ford ML, Evavold BD (2005) Specificity, magnitude, and kinetics of MOG-specific CD8$^+$ T cell responses during experimental autoimmune encephalomyelitis. Eur J Immunol 35:76–85. CrossRef Medline

Friese MA, Fugger L (2009) Pathogenic CD8(+) T cells in multiple sclerosis. Ann Neurol 66:132–141. CrossRef Medline

Friese MA, Jakobsen KB, Friis L, Etzensperger R, Craner MJ, McMahon RM, Jensen LT, Huygelen V, Jones EY, Bell JI, Fugger L (2008) Opposing effects of HLA class I molecules in tuning autoreactive CD8$^+$ T cells in multiple sclerosis. Nat Med 14:1227–1235. CrossRef Medline

Heim N, Garaschuk O, Friedrich MW, Mank M, Milos RI, Kovalchuk Y, Konnerth A, Griesbeck O (2007) Improved calcium imaging in transgenic mice expressing a troponin C-based biosensor. Nat Methods 4:127–129. CrossRef Medline

Höftberger R, Aboul-Enein F, Brueck W, Lucchinetti C, Rodriguez M, Schmidbauer M, Jellinger K, Lassmann H (2004) Expression of major histocompatibility complex class I molecules on the different cell types in multiple sclerosis lesions. Brain Pathol 14:43–50. CrossRef Medline

Hu D, Ikizawa K, Lu L, Sanchirico ME, Shinohara ML, Cantor H (2004) Analysis of regulatory CD8 T cells in Qa-1-deficient mice. Nat Immunol 5:516–523. CrossRef Medline

Huseby ES, Liggitt D, Brabb T, Schnabel B, Ohlén C, Goverman J (2001) A pathogenic role for myelin-specific CD8$^+$ T cells in a model for multiple sclerosis. J Exp Med 194:669–676. CrossRef Medline

Huseby ES, Huseby PG, Shah S, Smith R, Stadinski BD (2012) Pathogenic CD8 T cells in multiple sclerosis and its experimental models. Front Immunol 3:64. Medline

Jacobsen M, Cepok S, Quak E, Happel M, Gaber R, Ziegler A, Schock S, Oertel WH, Sommer N, Hemmer B (2002) Oligoclonal expansion of memory CD8$^+$ T cells in cerebrospinal fluid from multiple sclerosis patients. Brain 125:538–550. CrossRef Medline

Jiang H, Curran S, Ruiz-Vazquez E, Liang B, Winchester R, Chess L (2003) Regulatory CD8$^+$ T cells fine-tune the myelin basic protein-reactive T cell receptor V beta repertoire during experimental autoimmune encephalomyelitis. Proc Natl Acad Sci U S A 100:8378–8383. CrossRef Medline

Ji Q, Perchellet A, Goverman JM (2010) Viral infection triggers central nervous system autoimmunity via activation of CD8$^+$ T cells expressing dual TCRs. Nat Immunol 11:628–634. CrossRef Medline

Kerschensteiner M, Schwab ME, Lichtman JW, Misgeld T (2005) *In vivo* imaging of axonal degeneration and regeneration in the injured spinal cord. Nat Med 11:572–577. CrossRef Medline

Kim SM, Bhonsle L, Besgen P, Nickel J, Backes A, Held K, Vollmer S, Dornmair K, Prinz JC (2012) Analysis of the paired TCR α- and β-chains of single human T cells. PloS One 7:e37338. CrossRef Medline

Krishnamoorthy G, Wekerle H (2009) EAE: an immunologist's magic eye. Eur J Immunol 39:2031–2035. CrossRef Medline

Kuhn JR, Poenie M (2002) Dynamic polarization of the microtubule cytoskeleton during CTL-mediated killing. Immunity 16:111–121. CrossRef Medline

Leuenberger T, Paterka M, Reuter E, Herz J, Niesner RA, Radbruch H, Bopp T, Zipp F, Siffrin V (2013) The role of CD8$^+$ T cells and their local interaction with CD4$^+$ T cells in myelin oligodendrocyte glycoprotein35–55-induced experimental autoimmune encephalomyelitis. J Immunol 191:4960–4968. CrossRef Medline

Mank M, Santos AF, Direnberger S, Mrsic-Flogel TD, Hofer SB, Stein V, Hendel T, Reiff DF, Levelt C, Borst A, Bonhoeffer T, Hübener M, Griesbeck O (2008) A genetically encoded calcium indicator for chronic in vivo two-photon imaging. Nat Methods 5:805–811. CrossRef Medline

Marangoni F, Murooka TT, Manzo T, Kim EY, Carrizosa E, Elpek NM, Mempel TR (2013) The transcription factor NFAT exhibits signal memory during serial T cell interactions with antigen-presenting cells. Immunity 38:237–249. CrossRef Medline

Medana I, Martinic MA, Wekerle H, Neumann H (2001) Transection of major histocompatibility complex class I-induced neurites by cytotoxic T lymphocytes. Am J Pathol 159:809–815. CrossRef Medline

Meuth SG, Herrmann AM, Simon OJ, Siffrin V, Melzer N, Bittner S, Meuth P, Langer HF, Hallermann S, Boldakowa N, Herz J, Munsch T, Landgraf P, Aktas O, Heckmann M, Lessmann V, Budde T, Kieseier BC, Zipp F, Wiendl H (2009) Cytotoxic CD8$^+$ T cell-neuron interactions: perforin-dependent electrical silencing precedes but is not causally linked to neuronal cell death. J Neurosci 29:15397–15409. CrossRef Medline

Mitaksov V, Truscott SM, Lybarger L, Connolly JM, Hansen TH, Fremont DH (2007) Structural engineering of pMHC reagents for T cell vaccines and diagnostics. Chem Biol 14:909–922. CrossRef Medline

Moreau HD, Lemaître F, Terriac E, Azar G, Piel M, Lennon-Dumenil AM, Bousso P (2012) Dynamic in situ cytometry uncovers T cell receptor signaling during immunological synapses and kinapses in vivo. Immunity 37:351–363. CrossRef Medline

Na SY, Hermann A, Sanchez-Ruiz M, Storch A, Deckert M, Hünig T (2012) Oligodendrocytes enforce immune tolerance of the uninfected brain by purging the peripheral repertoire of autoreactive CD8$^+$ T cells. Immunity 37:134–146. CrossRef Medline

Neumann H, Cavalié A, Jenne DE, Wekerle H (1995) Induction of MHC class I genes in neurons. Science 269:549–552. CrossRef Medline

Neumann H, Boucraut J, Hahnel C, Misgeld T, Wekerle H (1996) Neuronal control of MHC class II inducibility in rat astrocytes and microglia. Eur J Neurosci 8:2582–2590. CrossRef Medline

Neumann H, Medana IM, Bauer J, Lassmann H (2002) Cytotoxic T lymphocytes in autoimmune and degenerative CNS diseases. Trends Neurosci 25:313–319. CrossRef Medline

Nikić I, Merkler D, Sorbara C, Brinkoetter M, Kreutzfeldt M, Bareyre FM, Brück W, Bishop D, Misgeld T, Kerschensteiner M (2011) A reversible form of axon damage in experimental autoimmune encephalomyelitis and multiple sclerosis. Nat Med 17:495–499. CrossRef Medline

Nitsch R, Pohl EE, Smorodchenko A, Infante-Duarte C, Aktas O, Zipp F (2004) Direct impact of T cells on neurons revealed by two-photon microscopy in living brain tissue. J Neurosci 24:2458–2464. CrossRef Medline

Nylander A, Hafler DA (2012) Multiple sclerosis. J Clin Invest 122:1180–1188. CrossRef Medline

Perchellet A, Stromnes I, Pang JM, Goverman J (2004) CD8$^+$ T cells maintain tolerance to myelin basic protein by 'epitope theft'. Nat Immunol 5:606–614. CrossRef Medline

Petermann F, Korn T (2011) Cytokines and effector T cell subsets causing autoimmune CNS disease. FEBS Lett 585:3747–3757. CrossRef Medline

Sandalova T, Michaëlsson J, Harris RA, Odeberg J, Schneider G, Kärre K, Achour A (2005) A structural basis for CD8$^+$ T cell-dependent recognition of non-homologous peptide ligands: implications for molecular mimicry in autoreactivity. J Biol Chem 280:27069–27075. CrossRef Medline

Saxena A, Bauer J, Scheikl T, Zappulla J, Audebert M, Desbois S, Waisman A, Lassmann H, Liblau RS, Mars LT (2008) Cutting edge: Multiple sclerosis-like lesions induced by effector CD8 T cells recognizing a sequestered antigen on oligodendrocytes. J Immunol 181:1617–1621. CrossRef Medline

Shakhar G, Lindquist RL, Skokos D, Dudziak D, Huang JH, Nussenzweig MC, Dustin ML (2005) Stable T cell-dendritic cell interactions precede the development of both tolerance and immunity in vivo. Nat Immunol 6:707–714. CrossRef Medline

Siewert K, Malotka J, Kawakami N, Wekerle H, Hohlfeld R, Dornmair K (2012) Unbiased identification of target antigens of CD8$^+$ T cells with combinatorial libraries coding for short peptides. Nat Med 18:824–828. CrossRef Medline

Siffrin V, Brandt AU, Herz J, Zipp F (2007) New insights into adaptive immunity in chronic neuroinflammation. Adv Immunol 96:1–40. CrossRef Medline

Siffrin V, Brandt AU, Radbruch H, Herz J, Boldakowa N, Leuenberger T, Werr J, Hahner A, Schulze-Topphoff U, Nitsch R, Zipp F (2009) Differential immune cell dynamics in the CNS cause CD4$^+$ T cell compartmentalization. Brain 132:1247–1258. CrossRef Medline

Siffrin V, Radbruch H, Glumm R, Niesner R, Paterka M, Herz J, Leuenberger T, Lehmann SM, Luenstedt S, Rinnenthal JL, Laube G, Luche H, Lehnardt S, Fehling HJ, Griesbeck O, Zipp F (2010) In vivo imaging of partially reversible th17 cell-induced neuronal dysfunction in the course of encephalomyelitis. Immunity 33:424–436. CrossRef Medline

Skokos D, Shakhar G, Varma R, Waite JC, Cameron TO, Lindquist RL, Schwickert T, Nussenzweig MC, Dustin ML (2007) Peptide-MHC potency governs dynamic interactions between T cells and dendritic cells in lymph nodes. Nat Immunol 8:835–844. CrossRef Medline

Somersalo K, Anikeeva N, Sims TN, Thomas VK, Strong RK, Spies T, Lebedeva T, Sykulev Y, Dustin ML (2004) Cytotoxic T lymphocytes form an antigen-independent ring junction. J Clin Invest 113:49–57. CrossRef Medline

Sun D, Wekerle H (1986) Ia-restricted encephalitogenic T lymphocytes mediating EAE lyse autoantigen-presenting astrocytes. Nature 320:70–72. CrossRef Medline

Sun D, Whitaker JN, Huang Z, Liu D, Coleclough C, Wekerle H, Raine CS (2001) Myelin antigen-specific CD8$^+$ T cells are encephalitogenic and produce severe disease in C57BL/6 mice. J Immunol 166:7579–7587. CrossRef Medline

Sun D, Zhang Y, Wei B, Peiper SC, Shao H, Kaplan HJ (2003) Encephalitogenic activity of truncated myelin oligodendrocyte glycoprotein (MOG) peptides and their recognition by CD8$^+$ MOG-specific T cells on oligomeric MHC class I molecules. Int Immunol 15:261–268. CrossRef Medline

Townsend A, Bastin J, Bodmer H, Brownlee G, Davey J, Gotch F, Gould K, Jones I, McMichael A, Rothbard J (1989) Recognition of influenza virus proteins by cytotoxic T lymphocytes. Philos Trans R Soc Lond B Biol Sci 323:527–533. CrossRef Medline

Zipp F, Aktas O (2006) The brain as a target of inflammation: common pathways link inflammatory and neurodegenerative diseases. Trends Neurosci 29:518–527. CrossRef Medline